



HAL
open science

Dissolved organic matter concentration and composition discontinuity at the peat-pool interface in a boreal peatland

Antonin Prijac, Laure Gandois, Laurent Jeanneau, Pierre Taillardat, Michelle Garneau

► To cite this version:

Antonin Prijac, Laure Gandois, Laurent Jeanneau, Pierre Taillardat, Michelle Garneau. Dissolved organic matter concentration and composition discontinuity at the peat-pool interface in a boreal peatland. *Biogeo-science*, 2022, 19 (18), pp.4571-4588. <10.5194/bg-19-4571-2022>. <insu-03783949>

HAL Id: insu-03783949

<https://insu.hal.science/insu-03783949v1>

Submitted on 22 Sep 2022

HAL is a multi-disciplinary open access archive for the deposit and dissemination of scientific research documents, whether they are published or not. The documents may come from teaching and research institutions in France or abroad, or from public or private research centers.

L'archive ouverte pluridisciplinaire HAL, est destinée au dépôt et à la diffusion de documents scientifiques de niveau recherche, publiés ou non, émanant des établissements d'enseignement et de recherche français ou étrangers, des laboratoires publics ou privés.



Distributed under a Creative Commons CC BY 4.0 - Attribution - International License



Dissolved organic matter concentration and composition discontinuity at the peat–pool interface in a boreal peatland

Antonin Prijac^{1,2,3}, Laure Gandois⁴, Laurent Jeanneau⁶, Pierre Taillardat^{1,7}, and Michelle Garneau^{1,2,3,5}

¹Centre de Recherche sur la Dynamique du Système Terre (GÉOTOP), Université du Québec à Montréal, Montréal, Canada

²Groupe de Recherche Inter-universitaire en Limnologie (GRIL), Université du Québec à Montréal, Montréal, Canada

³Institut des Sciences de l'Environnement (ISE), Université du Québec à Montréal, Montréal, Canada

⁴Laboratoire Géosciences Rennes, Université de Rennes, CNRS, UMR 6118, 35000 Rennes, France

⁵Département de Géographie, Université du Québec à Montréal, Montréal, Canada

⁶Laboratoire Géosciences Rennes, UMR 6118, CNRS-Université de Rennes, Rennes, France

⁷Integrated Tropical Peatlands Research Program (INTPREP), National University of Singapore, Singapore

Correspondence: Antonin Prijac (antonin.prijac@gmail.com) and Laure Gandois (laure.gandois@cnsr.fr)

Received: 13 March 2022 – Discussion started: 24 March 2022

Revised: 4 August 2022 – Accepted: 30 August 2022 – Published: 22 September 2022

Abstract. Pools are common features of peatlands and can represent from 5 % to 50 % of the peatland ecosystem's surface area. Pools play an important role in the peatland carbon cycle by releasing carbon dioxide and methane to the atmosphere. However, the origin of this carbon is not well constrained. A hypothesis is that the majority of the carbon emitted from pools predominantly originates from mineralized allochthonous (i.e., plant-derived) dissolved organic matter (DOM) from peat rather than in situ primary production. To test this hypothesis, this study examined the origin, composition, and degradability of DOM in peat porewater and pools of an ombrotrophic boreal peatland in northeastern Quebec (Canada) for 2 years over the growing season. The temporal evolution of dissolved organic carbon (DOC) concentration, the optical properties, molecular composition (THM-GC-MS), stable isotopic signature ($\delta^{13}\text{C}$ -DOC), and degradability of DOM were determined. This study demonstrates that DOM, in both peat porewater and pools, presents a diverse composition and constitutes highly dynamic components of peatland ecosystems. The molecular and isotopic analyses showed that DOM in pools was derived from plants. However, DOM compositions in the two environments were markedly different. Peat porewater DOM was more aromatic, with a higher molecular weight and DOC: DON (dissolved organic nitrogen) ratio compared to pools. The temporal dynamics of DOC concentration and DOM composition also differed. In peat porewater, the DOC concentration followed

a strong seasonal increase, starting from 9 mg L^{-1} and reaching a plateau above 20 mg L^{-1} in summer and autumn. This was explained by seasonal peatland vegetation productivity, which is greater than microbial DOM degradation. In pools, DOC concentration also increased but remained 2 times lower than in the peat porewaters at the end of the growing season ($\sim 10\text{ mg L}^{-1}$). Those differences might be explained by a combination of physical, chemical, and biological factors. The limited hydraulic conductivity in deeper peat horizons and associated DOM residence time might have favored both DOM microbial transformation within the peat and the interaction of DOM aromatic compounds with the peat matrix, explaining part of the shift of DOM compositions between peat porewater and pools. This study did not report any photolability of DOM and only limited microbial degradability. Thus, it is likely that the DOM might have been microbially transformed at the interface between peat and pools. The combination of DOM quantitative and qualitative analyses presented in this study demonstrates that most of the carbon present within and released from the pools originates from peat vegetation. These results demonstrate that pools represent a key component of the peatland ecosystem ecological and biogeochemical functioning.

1 Introduction

Northern peatlands constitute one of the most important terrestrial reservoirs of organic carbon (C) containing about 530 ± 160 Pg C while only covering $\sim 3\%$ of the global terrestrial land surface (Yu, 2012). The ecosystem carbon accumulation rates of peatlands are typically greater than the losses to the atmosphere through peat degradation and lateral transfer (Billett et al., 2006, 2012; Blodau et al., 2007; Tunaley et al., 2017). Peatlands are characterized by a mosaic of surface microforms, such as hummocks, lawns, hollows, and pools (Charman, 2002). Considering peatlands as a patchwork of microforms rather than a homogeneous ecosystem is critical to accurately quantify their carbon balance and the role they play in the modern global carbon cycle. Carbon dynamics between microforms are closely related to the vegetation type and water table depth, which influence the carbon dioxide (CO₂) and methane (CH₄) exchange with the atmosphere (Nungesser, 2003; Chaudhary et al., 2018). Among the different microforms, pools can constitute an important proportion of peatland ecosystem surface areas, ranging from 5% to 50% (White, 2011; Pelletier et al., 2014, 2015), and represent a net carbon source to the atmosphere (Pelletier et al., 2014). While most studies of peatland carbon dynamics have focused on terrestrial microforms (Nungesser, 2003; Pelletier et al., 2011; Shi et al., 2015; Chaudhary et al., 2018; Graham et al., 2020), the composition and processes of production and degradation of organic carbon in pools remain poorly documented.

The composition of dissolved organic matter (DOM) has previously been documented in peatland porewater. A complex mixture of compounds with a diversity of composition, functional groups, and ages seem to coexist (Tipping et al., 2010; Kaplan and Cory, 2016; Raymond and Spencer, 2015; Tiwari et al., 2018; Dean et al., 2019; Tfaily et al., 2018). The production of DOM in peat porewater is controlled by vegetation productivity, peat temperature (Rydin et al., 2013; Kane et al., 2014), and microbial activity (Worrall et al., 2008).

It has also been shown that pools can represent active compartments of peatland ecosystems for DOM (Laurion and Mladenov, 2013; Deshpande et al., 2016; Payandi-Rolland et al., 2020; Folhas et al., 2020; Laurion et al., 2021) – a topic that has been less studied. The DOM of pools may derive from surrounding terrestrial peat (i.e., allochthonous) or be the result of their internal primary production through phytoplankton and microbial production (i.e., autochthonous). In both peat porewater and pools, DOM is affected by biodegradation processes and by photodegradation in pools (Lapierre and del Giorgio, 2014; Vonk et al., 2015). Changes in dissolved organic carbon (DOC) concentrations and DOM composition are commonly observed and associated with a wide range of degradation rates (Frey et al., 2016; Payandi-Rolland et al., 2020; Moody and Worrall, 2021). The composition and reactivity of DOM transferred from the terrestrial

to aquatic compartments of peatlands highly depend on the hydrology and hydroclimatic context, as well as the biological and chemical processes occurring during their transfer (Jaffé et al., 2012; Kaplan and Cory, 2016). The DOM transfers between peatlands and aquatic ecosystems are well documented for streams (Elder et al., 2000; Billett et al., 2006, 2012; Austnes et al., 2010; Knorr, 2013; Frey et al., 2016; Buzek et al., 2019; Dean et al., 2019; Rosset et al., 2019) but more rarely for pools (Banae, 2013; Arsenault et al., 2019; Payandi-Rolland et al., 2020).

Differences in DOM composition and concentration between peat porewater and pools have been observed, but the processes involved remain unclear (Schindler et al., 1997; Payandi-Rolland et al., 2020). Studies conducted in temperate peatlands have highlighted that the morphology (e.g., size, shape, depth, and slope of banks) and surrounding vegetation influence the carbon content and hydrochemistry in the pools (Banae, 2013; Arsenault et al., 2018, 2019). Others have explained the changes in DOM composition in pools as the result of photodegradation and biodegradation (Laurion and Mladenov, 2013; Arsenault et al., 2019; Laurion et al., 2021). Studies investigating the changes in DOM composition in peatland porewater and pools have mostly been focused on temperate (Banae, 2013; Arsenault et al., 2019), subarctic, and Arctic regions (Laurion and Mladenov, 2013; Deshpande et al., 2016; Burd et al., 2020; Payandi-Rolland et al., 2020; Laurion et al., 2021; Moody and Worrall, 2021), but there is no insight about changes in DOM compositions in boreal peatlands not affected by permafrost.

Because DOM may derive from different sources and be subjected to various processes of transformation and degradation, apprehending the complexity of the origin, composition, and properties of the molecules that compose the DOM is challenging. The use of complementary analytical methods is a good approach to characterize DOM and attempt to understand its origin and composition (Folhas et al., 2020; Tfaily et al., 2013). The DOC:DON (dissolved organic nitrogen) elementary ratio is used to estimate the extent of microbial processing of DOM (McKnight et al., 1994; Autio et al., 2016). The absorbance and fluorescence are recognized tools to estimate the average DOM molecular weight and aromaticity (Haan and Boer, 1987; Weishaar et al., 2003; Helms et al., 2008), discriminate the origin of DOM between microbial and plant sources (McKnight et al., 2001; Cory et al., 2010), and highlight microbial degradation (Parlanti, 2000; Wilson and Xenopoulos, 2009). The stable carbon isotopic signature of DOC ($\delta^{13}\text{C}$ -DOC) can be used to discriminate between terrestrial and aquatic plant-derived DOM and also the extent of microbial processing of DOM (Elder et al., 2000; Billett et al., 2012; Buzek et al., 2019). Finally, the analysis of target molecules using THM-GC-MS allows the definition of indicators of DOM sources and processing degradation stage (Jeanneau et al., 2014, 2015; Kaal et al., 2017, 2020).

The aim of this study is to clarify the role that pools play in the production, transfer, and transformation of organic carbon within peatland ecosystems. We identified three possible scenarios. First, pools are mineralization hotspots that can decompose the laterally exported fresh organic matter from adjacent peat porewater. Second, pools represent passive pipes that only collect the remaining refractory DOM laterally exported from peat porewater. Third, pools represent a sub-ecosystem within the peatland where both primary productivity and heterotrophic respiration exist. To determine which scenario is the most accurate, we studied the spatiotemporal variability of DOM over two growing seasons in a boreal ombrotrophic peatland. The objectives of this study were to (i) identify the differences in the origin, quantity, composition, and degradability of DOM between peat porewater and pools; (ii) understand which factors induce those differences; and (iii) clarify the contribution of DOM in pools to the peatland carbon cycle.

2 Study site

The study site is located in northeastern Quebec, Canada, within the Romaine River watershed (14 500 km²), adjacent to the Labrador border. It is located in the eastern spruce–moss bioclimatic domain of the closed boreal forest (Payette, 2001) at the limit of the coastal plain and the Highlands of the Laurentian Plateau of the Precambrian Shield (Dubois, 1980). The Bouleau peatland (unofficial name; 50°31′ N, 63°12′ W; altitude 108 ± 5 m) is an ombrotrophic, slightly dome-shaped bog with a total surface area of 1.18 km² (Tailardat et al., 2022). Peat accumulation was initiated at ca. 9260 cal BP, and the maximum peat depth reaches 440 cm (Primeau and Garneau, 2021). The mean annual temperature is 1.5 °C, and the mean annual precipitation is 1011 mm, of which 590 mm falls as snow. The average monthly positive temperatures occur from May to October with 1915 growing degree days above 0 °C (Havre-Saint-Pierre meteorological station, mean 1990–2019; Meteorological Service of Canada and Environment and Climate Change Canada, 2019).

The surface microforms of the Bouleau peatland show a clear patterned surface of alternating dry hummocks, lawns, hollows, and pools. The surface vegetation varies according to the microtopography with *Sphagnum fuscum*, *S. capillifolium*, and *Cladonia rangiferina* on hummocks; *S. magellanicum*, *S. rubellum*, *S. cuspidatum*, and *Trichophorum cespitosum* on lawns; and *S. majus* and *S. pulchrum* on hollows (Primeau and Garneau, 2021). Pools cover 9 % of the peatland surface area and are characterized by their elliptical morphology, steep banks, and slightly concave bottoms. Because of the steep banks, no aquatic vegetation is observed along the edges of the pools.

3 Material and methods

3.1 Water sampling

Sampling was performed five times during the 2018 growing season (June, July, August, September, and October) and four times in 2019 (June, August, September, and October).

The peat porewater was sampled from six wells (P1 to P6, Fig. 1) located along a topographic transect from the dome to the southern edge of the peatland. Two meters long PVC wells were perforated and covered with a nylon sock to avoid infilling by peat. They were inserted in peat to collect water in the first 2 m of the peat column. This method allows collecting the fluctuating water table which moves through the peat. In 2018, six pools were chosen along a north–south axis giving a distance gradient to the stream outlet (M01 to M06, Fig. 1). In 2019, the pools were divided into five class sizes, and one pool was chosen into each class (M11 to M15, Fig. 1). The pool sizes varied from 30 to 2065 m² with a mean depth between 70 and 120 cm. Pools were sampled from their banks and from the surface of the water column.

The physicochemical parameters (temperature, pH, specific conductivity, and dissolved oxygen saturation) of peat porewater and pool water were measured using a multi-parameter portable meter (MultiLine Multi 3620 IDS, WTW, Germany) at each sampling site and calibrated before each field visit. All water samples were collected in clean polypropylene (PP) bottles and filtered on pre-combusted (4h at 450 °C) GF/F filters (Whatman). Samples collected during each field campaign and analyses performed are synthesized in Table S1 in the Supplement.

3.2 Water-level and temperature monitoring

3.2.1 Instrumentation

The six wells were equipped with a water-level data logger U20-001-04 in 2018 and replaced with a U20I-04 in 2019 (HOBO, Onset, USA) for continuous measurements of the water table depth (WTD) and temperature from June 2018 to October 2020. Water temperature was recorded hourly in pools M11 to M15 using HOBO TMC50 probes coupled with a HOBO U12-008 data logger (Onset, USA) from June 2019 to August 2020. A water-level data logger was installed in pool M11 (Fig. 1), and water-level variations were measured from 20 May to 28 August 2020. Height variations (in cm) between the peatland surface at wells P5 and P6 and adjacent pool M11 were measured using a ZIPLEVEL Pro-2000 (Technidea, USA). Those measurements allowed the water levels in the pool to be compared with those in the two wells (Fig. S2 in the Supplement). An EXO2 multiparameter probe (YSI, USA) was installed at the outlet of the peatland stream to record water temperature hourly, from June 2018 to August 2020.

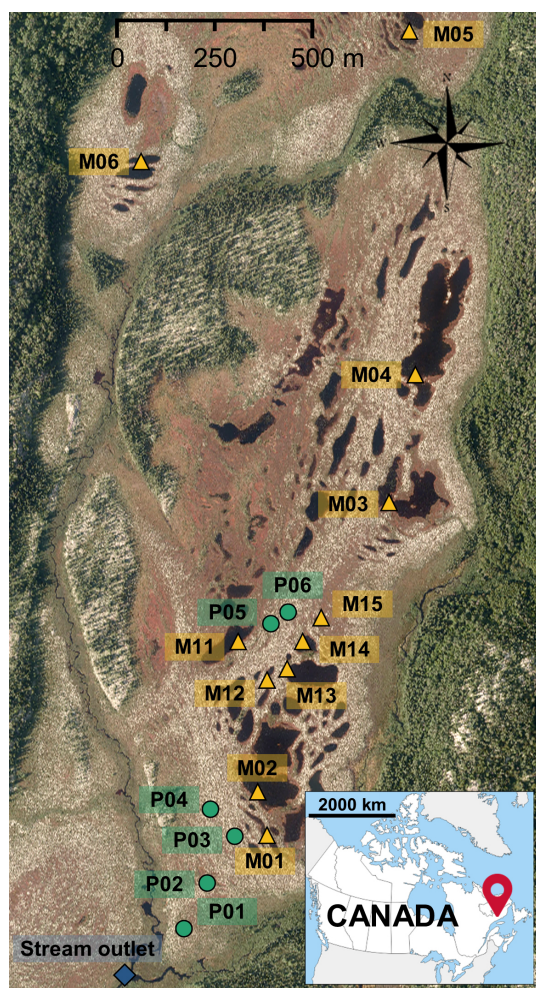


Figure 1. Aerial view of the Bouleau peatland with the location of the sampling sites (green dots: wells for peat porewater; yellow triangles: pools; blue diamond: stream outlet). The aerial photo was provided by Hydro-Québec.

3.2.2 Season definition

Samples from the 2 studied years were pooled according to seasons. In this study, seasons were defined based on air and water temperatures measured at the site (Fig. S3). Spring was defined by the end of the seasonal thaw that occurred in May to the end of June. Summer included the months of July and August when air and water temperatures were at their warmest. Finally, the autumn season corresponded to the months of September and October when air and water temperature decreased to zero.

3.2.3 Quantitative analyses

The filtered water samples (through GF/F filters) were prepared for DOC and total nitrogen (TN) analyses by acidification to pH 2 with 1 M HCl and stored in 40 mL glass vials. The DOC and TN concentrations were analyzed using the

catalytic oxidation method followed by the non-dispersive infrared (NDIR) detection of the CO₂ produced (TOC analyzer TOC-L, Shimadzu, Japan) with limits of quantification of 0.1 mg C L⁻¹ and 0.2 mg N L⁻¹.

The samples were prepared for cation and anion analyses and stored in high-density polyethylene (HDPE) vials without acidification. Those ions (chloride, ammonium, nitrites, and nitrates) were analyzed by high-performance liquid chromatography (HPLC) coupled with a Dionex ICS-5000+ analyzer for anions (Thermo Fisher Scientific) and a Dionex DX-120 analyzer for cations (Thermo Fisher Scientific).

The reference materials included ION-915 and ION 96.4 (Environment and Climate Change Canada, Canada). The analyses were performed at EcoLab (UMR 5245 CNRS – UT3 – INPT, France).

Dissolved organic nitrogen (DON) corresponds to the difference between the concentration of TN and the sum of concentration of inorganic nitrogen (ammonium, nitrites, and nitrates).

3.3 Qualitative analyses

3.3.1 Stable isotopic analyses

Analyses of δ¹³C-DOC were realized on 41 samples selected from peat porewater (*n* = 20) and pools (*n* = 21; Table S1) at the Ján Veizer stable isotope laboratory (University of Ottawa, Canada) following the method developed by Lalonde et al. (2014). The samples were acidified to pH 2 with 1 M HCl and stored in 40 mL quality certified ultra-clean borosilicate glass vials. The first step involved the catalytic oxidation of DOC followed by a solid-state non-dispersive infrared (SS-NDIR) detection of the CO₂ produced (OI Aurora 1030C, Xylem Analytics, USA). The produced CO₂ was passed through a chemical trap and a Nafion trap prior to ¹³C isotopic analyses using isotope-ratio mass spectroscopy (IRMS, Thermo Finnigan DeltaPlus XP, Thermo Electron Corporation, USA). The results were standardized with organic standards (KHP and sucrose), and the ¹³C/¹²C ratios were expressed as per mill deviations from the international standard VPDB.

3.3.2 Optical analyses

The samples for ultraviolet–visible spectroscopy analyses were stored at 4 °C in glass vials following filtration on GF/F filters. The absorbance was measured from 180 to 900 nm with a 5 nm resolution. The absorbance analyses were performed on an Ultrospec 3100 instrument (Biochrom, United Kingdom) for 2018 samples and on a Duetta instrument (Horiba, Japan) for 2019 samples, over a wavelength range from 190 to 900 nm at 2 nm intervals. All analyses were performed at the GRIL laboratory (GRIL, UQAM, Canada). For comparison, 10 samples from the 2019 campaign were randomly selected and analyzed on both instruments, Duetta and

Ultrospec 3100. A pairwise *t* test revealed slight but significant differences between absorbance at 254 nm from the two series ($t = -3.9013$, $df = 9$, p value = 0.0036). As no significant effect was observed between years on absorbance indices, no correction was performed on absorbance spectra.

The absorbance indices were calculated to provide information about DOM composition. Those indices were $SUVA_{254}$ ($L\ mg^{-1}\ m^{-1}$), which is a proxy of the DOM's aromatic content (Weishaar et al., 2003); $E2 : E3$ ratio; and spectral slope ratio (S_R), which are proxies of the average DOM molecular weight (Haan and Boer, 1987; Helms et al., 2008).

In 2019, spectrofluorometric analyses were also conducted on Duetta (Horiba, Japan) at the GRIL laboratory. Samples were excited at a range from 230 to 450 nm (at 2 nm resolution), and fluorescence was measured at a range from 240 to 600 nm (at a 5 nm resolution). Prior to the analyses, the samples were diluted when necessary to maintain an absorbance intensity at 254 nm below 0.6. A blank sample with Milli-Q water (Merck Millipore, Germany) was measured prior to the sample analyses. The sample spectra were obtained by subtracting the blank spectra to eliminate the Raman scatter peak. The operation was conducted automatically by the analytical equipment.

Two indices were calculated to provide qualitative information on the fluorescent fraction of the DOM: the fluorescence index (FI), lower values ($FI \approx 1.4$) of which indicate a plant origin while higher values ($FI \approx 1.9$) indicate a microbial origin of DOM (Cory et al., 2010; McKnight et al., 2001); and the $\beta : \alpha$ index, which is known as a proxy of biological activity, and an increase in the ratio of which corresponds to an increasing proportion of the recently produced DOM derived from microbial activity (Parlanti, 2000; Wilson and Xenopoulos, 2009).

3.3.3 Molecular analyses

Thermally assisted hydrolysis methylation–gas chromatography–mass spectrometry (THM-GC-MS) was performed on 37 samples from peat porewater ($n = 18$) and pools ($n = 19$; Table S1). Those samples were selected to include summer and autumn 2018 and spring, summer, and autumn 2019. The THM-GC-MS analyses were conducted on freeze-dried samples from 100 mL of water previously filtered on GF/F filters (Whatman) and followed the procedure described by Jeanneau et al. (2015). One milligram of the sample was introduced into an 80 μ L stainless-steel reactor with an excess of tetramethylammonium hydroxide (6 mg). The THM reaction was performed at 400 °C using a vertical microfurnace pyrolyzer PZ-2020D (Frontier Laboratories, Japan). The reaction products were injected into a gas chromatograph GC-2010 (Shimadzu, Japan) equipped with an SLB-5ms capillary column in split mode (60 m \times 0.25 mm i.d., 0.25 μ m film thickness). The compounds were detected with a mass spectrometer QP2010+ (Shimadzu, Japan)

operating in full scan mode. Analyses were realized at the Géosciences Rennes laboratory (UMR 6118 – Univ. Rennes – CNRS, France).

For each chromatogram, the compounds were identified based on known m/z ratios (Table S1) through comparison with the NIST library. The area of each compound was integrated for each m/z and corrected by a mass spectra factor (MSF). The MSF corresponds to the reciprocal of the integrated fragment proportion and the entire related fragmentogram in the NIST library. The relative proportion of each compound was calculated by dividing the compound area (for all cumulated peaks) by the sum of total integrated compound areas and expressed as a percentage.

All compounds were classified into five groups, and their relative proportions were calculated: %CAR of carbohydrates compounds (derived from both plant and microbial metabolism), %LMW_FA for low-molecular-weight fatty acids (derived from microbial metabolism), %HMW_FA for high-molecular-weight fatty acids, %SOA for small organic acids, and %Phenols for phenol markers (derived from plant metabolism). The indices were calculated for each sample, derived from molecular analyses, and presented as in Jeanneau et al. (2015). The C/V ratio corresponds to the sum of coumaric and ferulic acids divided by the sum of vanillic acid, vanillaldehyde, and acetovanillone. The deoxyC6 : C5 ratio is a mixing model based on the proportion of deoxyC6 carbohydrates (derived mainly from microorganisms) and the proportion of C5 carbohydrates (derived mainly from plants). Values close to 0.5 suggested a dominant contribution of plant-derived DOM, while values close to 2 corresponded to the contribution of microbial-derived DOM (Rumpel and Dignac, 2006). The last index corresponds to the proportion of plant-derived markers, f_{VEG} , which is the difference between the total markers and the microbial-derived markers, f_{MIC} . The f_{MIC} corresponds to the proportion of microbial carbohydrates multiplied by the total proportion of carbohydrates, summed up by the proportion of microbial fatty acids, and multiplied by the total proportion of fatty acids. The MIC : VEG index corresponds to the ratio of microbial-derived markers divided by the proportion of plant-derived markers.

3.4 Incubation of dissolved organic matter

3.4.1 Experimental design

The objective of DOM incubation experiments was to test the sensitivity of DOM to biodegradation and photodegradation and how it could affect its composition. The incubation experiments were designed to test the effects of temperature (in situ versus controlled) and total organic carbon versus dissolved organic carbon on DOM degradation rates.

DOM from peat porewater and pools was incubated during three sampling periods in 2019, from 7 to 13 June, 31 July to 7 August, and 4 to 10 September. An incubation time

of 6 d had to be adjusted to 7 d during the last campaign due to logistical constraints. Pool M11 was used to monitor the water level using a barometric pressure sensor and was also sampled for incubations. The peat porewater samples consisted of a mix of equal water volumes between five different wells. This strategy was used because the water quantity in piezometers was limited and not sufficient to perform all incubation conditions.

The incubation experiments were performed on 100 mL of water filtered on GF/F filters (*F*) and in unfiltered (UF) conditions. Amber borosilicate glass vials of 125 mL were used to test biodegradation (BIO) only, and transparent borosilicate vials of 125 mL were used for biodegradation and photodegradation (BIO+PHOTO). Each condition was incubated in triplicates with a headspace of 25 mL, and bottles were tightly closed. Considering the absence of standardized incubation media between porewater and pools (Vonk et al., 2015), measured biodegradation rates could be dependent on the abundance and the activity of microorganisms in the samples from each environment.

For in situ incubations (IS), the peat porewater samples were placed 1–2 cm below the water surface at the outlet of the peatland (Fig. 1), where water temperature was recorded hourly with the EXO2 probe. The pool samples were placed 1–2 cm below the water surface of pool M11 (Fig. 1). For controlled conditions (CC), the vials were placed in a dark room in a laboratory space at Havre-Saint-Pierre, where the temperature was maintained between 18 and 20 °C and controlled twice each day. Both in situ and controlled conditions started the same day. There is no value available for *F* conditions in pools in August due to variability between the incubated water volume, suggesting that vial caps were loose.

3.4.2 Post-incubation analysis

In the end, samples incubated under UF conditions ($n = 18$) were filtered on a GF/F filter to analyze only the dissolved fraction. All samples ($n = 36$) were prepared for DOC, TN, and inorganic N quantification, as well as absorbance analyses, before and after the incubation experiments. The apparent removal rate of dissolved organic carbon (RDOC), expressed in milligrams per day (mg d^{-1}), corresponds to the amount of DOC removed during incubation, reported per day, and calculated following Eq. (1).

$$\text{RDOC (mg d}^{-1}\text{)} = \frac{([\text{DOC}]_{\text{pre-incubation}} - [\text{DOC}]_{\text{post-incubation}})}{\text{incubation time}}$$

$[\text{DOC}]_{\text{pre-incubation}}$ (mg L^{-1}):
 DOC concentration at the beginning of incubation
 $[\text{DOC}]_{\text{post-incubation}}$ (mg L^{-1}):
 DOC concentration at the end of incubation

(1)

The degradation rates correspond to the proportion of DOC lost per day of incubation and are expressed in percent of

carbon per day ($\% \text{C d}^{-1}$) according to Eq. (2).

$$\text{Degradation rate (}\% \text{C d}^{-1}\text{)} = \frac{([\text{DOC}]_{\text{pre-incubation}} - [\text{DOC}]_{\text{post-incubation}})}{[\text{DOC}]_{\text{pre-incubation}}} \times 100 / \text{incubation time}$$

(2)

Changes in the DOC:DON ratio and absorbance indices were determined in proportion to the initial values per day for the variable *i* following Eq. (3).

$$\Delta i (\text{d}^{-1}) = \frac{i_{\text{post-incubation}} - i_{\text{pre-incubation}}}{i_{\text{pre-incubation}}} / \text{incubation time}$$

(3)

Δi is the change of the variable *i* during the incubation, $i_{\text{pre-incubation}}$ is the initial value of the variable *i* at the beginning of incubation, and $i_{\text{post-incubation}}$ is the value of the variable *i* at the end of incubation.

3.5 Statistical analyses

All statistical tests were performed on R (CRAN project) through the RStudio interface (RStudio inc., USA), and all figures were realized with the package ggplot2 (Wickham, 2016).

Comparisons of variance tests were performed, and in the following sections, the mention of significant differences refers to statistical tests using the following method. First, normal distribution was tested using the Shapiro and Wilk test, and a normal distribution was considered true when the *p* value was >0.05 . If the distribution was not normal, a Kruskal and Wallis test was performed to compare the averages, and significant differences were considered true when the *p* value was <0.05 . Dunn tests were performed as post hoc pairwise comparison tests to determine which group was significantly different (when the *p* value <0.05). Second, the homogeneity of variance was tested using the Levene test and was considered true when the *p* value was >0.05 . If the homogeneity of variance was not true, a Welch ANOVA was performed, and significant differences were admitted when the *p* value was <0.05 . Estimated marginal means tests were performed as post hoc tests to determine significantly different groups (*p* value <0.05). In cases where the normal distribution and homogeneity of variances were true, an ANOVA was performed, and significant differences were true when the *p* value was <0.05 . When there were significant differences, the Tukey tests were performed as post hoc tests to determine which groups were significantly different (when the *p* value <0.05). The results of the statistical tests are summarized in Table S2.

Principal component analyses (PCAs) were used to explore relationships between DOM qualitative variables in peat porewater and pools. The selected variables were quantitative variables as DOC concentrations and qualitative variables as the DOC:DON ratio, optical indices

(SUVA₂₅₄, *E2* : *E3* ratio, and *S_R*), and molecular indices (deoxyC6 : C5, *f*VEG, *f*MIC, MIC : VEG ratio, *C*/*V* ratio, and Ac : Al(*V*) ratio), as well as molecular compound proportions (%SOA, %CAR, and %CAR_MIC, %LMW_FA, %HMW_FA, and %Phenols). Environmental and seasonal variables were used as supplementary qualitative variables. Prior to PCA, a correlation matrix was performed to identify strong correlations between the variables (Fig. S1). One of the correlated variables was excluded from PCA when the correlation was >0.90 or < -0.90, with *p* values <0.05. Therefore, the DOC : DON ratio (DOC : DON ~ DOC, *r* = 0.90, *p* value <0.0001), %CAR_MIC (%CAR_MIC ~ deoxyC6 : C5 ratio, *r* = 0.99, *p* value <0.0001), and *f*MIC (*f*MIC ~ MIC : VEG ratio, *r* = 0.98, *p* value <0.0001) were excluded from the PCA data set. The PCA was performed with the package FactoMineR (Lê et al., 2008). The ellipses in the representation of the first two axes of the PCA correspond to the function *addEllipses* from the R package FactoMineR used to add concentration ellipses to the plot.

4 Results

4.1 Hydrodynamics and physicochemical characteristics

Pool and peat water levels followed the same seasonal trend, although the water level in the pools was always lower than in peat. Thus, the preferential water flow goes from peat porewater to pools. The response of the water level to precipitation was slower and buffered in pools compared to peat (Fig. S2), and an average time lag of 13 h was measured between the WTD peak of peat and pools.

Peat porewater temperatures were constantly lower compared to pools, with 13.4 ± 4.4 °C in peat porewater against 17.1 ± 5.5 °C in pools when averaged over the two growing seasons. In both environments, the pH was acidic with an average of 4.9 ± 0.7 in peat porewater and 4.4 ± 0.3 in pools. Specific conductivity was on average almost 2 times higher in peat porewater than in pools, with 33.0 ± 19.3 and 14.0 ± 6.1 μS cm⁻¹ in peat porewaters and pools, respectively. Pool waters were characterized by their constant saturation in dissolved oxygen, with 99.9 ± 5.2 % saturation on average, while dissolved oxygen saturation was 50.04 ± 17.1 % saturation in peat porewater (Table 1).

4.2 Evolution of DOC concentrations and DOC : DON ratios

The DOC concentrations in peat porewater were significantly higher than in pools (Fig. 2a). In both environments, the DOC concentrations showed the same seasonal trends with a significant increase from spring to summer. The DOC concentrations increased significantly in peat porewater from 9.2 ± 4.2 mg L⁻¹ in spring, reaching a plateau

above 20 mg L⁻¹ during summer and autumn. In pools, the DOC concentrations also increased significantly from 7.5 ± 3.2 mg L⁻¹ in spring to a plateau above 10 mg L⁻¹ in summer and autumn.

Peat porewater presented a significantly higher DOC : DON ratio than pools. In both environments, the DOC : DON ratio increased significantly from spring to a plateau in summer and autumn (Fig. 2b). In peat porewater, the DOC : DON ratio increased from 32.3 ± 12.4 in spring to 52.8 ± 22.5 and 56.6 ± 8.2 in summer and autumn, respectively (Fig. 2b). In pools, the DOC : DON ratio increased from 26.2 ± 7.7 in spring to a plateau of 32.0 ± 7.5 in summer and 31.7 ± 6.6 in autumn.

4.3 Evolution of the isotopic compositions of DOM

Different trends for δ¹³C-DOC were identified between peat porewater and pools (Fig. 2c). In peat porewater, δ¹³C-DOC decreased significantly from spring, when the ratio was -26.0 ± 0.9 ‰, to autumn, when the ratio dropped to -27.5 ± 0.5 ‰. In pools, δ¹³C-DOC showed a nonsignificant increase from -27.5 ± 0.3 ‰ in spring to -26.8 ± 0.8 ‰ in autumn. In summer, δ¹³C-DOC was significantly different between peat porewater and pools.

4.4 Evolution of the optical and fluorescent properties of DOM

The DOM presented different optical properties between peat porewater and pools. Among those, SUVA₂₅₄ was significantly higher in porewater than in pools during the whole growing season, indicating a higher aromaticity of peat porewater DOM (Table 1). During the growing season, there were no major changes of SUVA₂₅₄ in peat porewater, but a slight increase was observed in pools during the autumn (Fig. 2d).

The *E2* : *E3* ratio was significantly higher in pools than in peat porewater, indicative of a lower average molecular weight. Compared to SUVA₂₅₄, the *E2* : *E3* ratio showed no significant trends in peat porewater, but it slightly increased in pools from 4.02 ± 0.11 in spring to 4.41 ± 0.18 in autumn, suggesting a decrease in the average molecular weight during the growing season (Fig. 2e).

The lower spectral slope ratio (*S_R*) of peat porewater DOM also suggested a higher molecular weight than in pool DOM. During the growing season, the *S_R* was steady in peat porewater with no significant changes between seasons, suggesting a homogeneity of the molecular weight of DOM (Fig. 2f). In pools, *S_R* values increased from spring to summer and decreased in autumn. Thus, according to the *S_R*, the lowest average molecular weight was reached during the summer in pools.

The fluorescence index (FI) was significantly higher in peat porewater than in pools but varied within a narrow range, close to typical terrestrial-derived organic matter (Fig. 2g). During the growing season, the index remained

Table 1. Peat porewater and pool seasonal average (\pm SD) of physicochemical variables (water temperature, pH, specific conductivity, and dissolved oxygen saturation), dissolved organic carbon (DOC) concentrations, and the ratio of DOC to dissolved organic nitrogen (DON) (DOC : DON), isotopic signature of DOC ($\delta^{13}\text{C}$ -DOC), optical indices (SUVA₂₅₄, $E2 : E3$ ratio, and spectral slope ratio), fluorescence indices (FI and $\beta : \alpha$ index), and molecular indices (f VEG, f MIC deoxyC6 : C5, and C/V ratio, as well as %Phenols, %CAR, %CAR_MIC, %SOA, %LMW_FA, and %HMW_FA).

	Peat porewater			Pools		
	Spring	Summer	Autumn	Spring	Summer	Autumn
Physicochemical parameters						
Water temperature ($^{\circ}\text{C}$)	12.3 \pm 5.2	16.5 \pm 2.3	11.8 \pm 4.2	14.8 \pm 1.7	22.8 \pm 2.9	13.7 \pm 4.9
pH	4.4 \pm 0.6	5.2 \pm 0.3	4.9 \pm 0.7	4.4 \pm 0.2	4.5 \pm 0.2	4.3 \pm 0.2
Conductivity ($\mu\text{S cm}^{-1}$)	41.7 \pm 23.9	26.1 \pm 7.4	33.5 \pm 21.7	8.39 \pm 1.7	12.1 \pm 3.5	19.1 \pm 5.5
Dissolved oxygen (% saturation)	56.0 \pm 16.2	45.3 \pm 16.8	50.4 \pm 17.5	101.0 \pm 2.9	102.0 \pm 5.8	97.5 \pm 4.9
Organic matter quantitative proxies						
DOC (mg L^{-1})	9.2 \pm 4.2	20.2 \pm 8.5	22.5 \pm 5.4	7.5 \pm 3.2	10.4 \pm 3.7	12.4 \pm 4.0
DOC : DON	32.3 \pm 12.4	52.8 \pm 22.5	56.6 \pm 8.2	26.2 \pm 7.7	32.0 \pm 7.5	31.7 \pm 6.6
DON (mg L^{-1})	0.29 \pm 0.1	0.39 \pm 0.08	0.39 \pm 0.06	0.29 \pm 0.1	0.39 \pm 0.11	0.39 \pm 0.09
Isotopic and optical indices						
$\delta^{13}\text{C}$ -DOC (‰)	-26.0 \pm 0.9	-27.3 \pm 0.3	-27.5 \pm 0.5	-27.5 \pm 0.3	-27.1 \pm 0.4	-26.8 \pm 0.8
SUVA ₂₅₄ ($\text{L mg}^{-1} \text{ m}^{-1}$)	6.0 \pm 1.5	5.13 \pm 0.5	5.55 \pm 1.0	2.88 \pm 1.5	3.13 \pm 0.5	3.86 \pm 0.6
$E2 : E3$ ratio	3.4 \pm 0.2	3.5 \pm 0.2	3.6 \pm 0.2	4.0 \pm 0.1	4.2 \pm 0.2	4.4 \pm 0.2
S_R	0.67 \pm 0.04	0.64 \pm 0.05	0.67 \pm 0.03	0.77 \pm 0.06	0.81 \pm 0.05	0.72 \pm 0.05
Fluorescence index	1.39 \pm 0.09	1.40 \pm 0.13	1.33 \pm 0.07	1.27 \pm 0.04	1.26 \pm 0.03	1.27 \pm 0.04
$\beta : \alpha$ index	0.63 \pm 0.10	0.65 \pm 0.08	0.59 \pm 0.05	0.62 \pm 0.03	0.69 \pm 0.07	0.61 \pm 0.07
Molecular indices and family compound proportions						
f VEG (%)	68.6 \pm 1.1	69.8 \pm 3.6	62.7 \pm 3.2	64.3 \pm 10.6	60.8 \pm 6.7	62.8 \pm 3.5
f MIC (%)	5.8 \pm 1.4	7.2 \pm 3.4	5.8 \pm 2.3	8.0 \pm 5.2	11.7 \pm 6.0	7.2 \pm 2.0
MIC : VEG ratio	0.09 \pm 0.02	0.10 \pm 0.05	0.09 \pm 0.04	0.14 \pm 0.13	0.20 \pm 0.12	0.12 \pm 0.04
deoxyC6 : C5	0.67 \pm 0.11	0.64 \pm 0.25	0.50 \pm 0.17	0.73 \pm 0.10	1.10 \pm 0.19	0.91 \pm 0.33
C/V	0.37 \pm 0.11	0.37 \pm 0.13	0.22 \pm 0.07	0.18 \pm 0.04	0.22 \pm 0.08	0.19 \pm 0.04
%Phenols (%)	57.6 \pm 6.3	54.1 \pm 9.2	53.6 \pm 4.6	59.0 \pm 10.1	53.3 \pm 8.5	54.6 \pm 7.9
%SOA (%)	19.9 \pm 0.4	18.1 \pm 5.8	26.6 \pm 6.3	21.5 \pm 3.9	20.4 \pm 4.7	24.5 \pm 3.5
%CAR (%)	7.3 \pm 1.6	5.7 \pm 3.2	6.7 \pm 5.2	4.6 \pm 2.2	8.8 \pm 9.4	7.8 \pm 6.6
%CAR_MIC (%)	0.11 \pm 0.08	0.11 \pm 0.15	0.05 \pm 0.07	0.15 \pm 0.07	0.40 \pm 0.13	0.28 \pm 0.22
%LMW_FA (%)	5.0 \pm 0.7	6.7 \pm 3.0	5.2 \pm 1.9	7.2 \pm 5.9	7.6 \pm 3.8	5.6 \pm 1.6
%HMW_FA (%)	4.6 \pm 4.4	10.6 \pm 8.6	3.00 \pm 3.3	1.4 \pm 0.1	2.9 \pm 1.3	2.1 \pm 1.0

steady in both environments with an average of 1.36 ± 0.10 in peat porewater against 1.27 ± 0.04 in pools.

The $\beta : \alpha$ index did not differ significantly between peat porewater and pools, where it was on average 0.62 ± 0.07 and 0.64 ± 0.07 , respectively (Fig. 2h). During the growing season, the index remained steady in peat porewater. In pools, the $\beta : \alpha$ index increased significantly from spring to summer: from 0.62 ± 0.03 to reaching a peak at 0.69 ± 0.07 . As the changes observed for the FI, variations of the $\beta : \alpha$ index were limited to a small range.

4.5 Evolution of the molecular composition of DOM

Phenol markers dominated (54 %) the molecular markers of DOM for both peat porewater and pools (Table 1). A simi-

lar proportion of small organic acids (22 % on average) was measured in both environments. Carbohydrates represented 6 % of the total markers in peat porewater and up to 8 % in pools. The distribution of fatty acids differed between the two environments. While low-molecular-weight fatty acids showed similar proportions in peat porewater (5.8 %) and pools (6.7 %), high-molecular-weight fatty acids, which are associated with plant inputs, were almost 3 times higher in peat porewater (6.1 %) than in pools (2.3 %).

In addition, three modifications of the molecular composition of DOM between the two environments must be highlighted. First, the C/V ratio (Fig. 2i), a lignin compositional proxy, was significantly higher in peat porewater than in pools (p value < 0.01). While it remained almost stable in

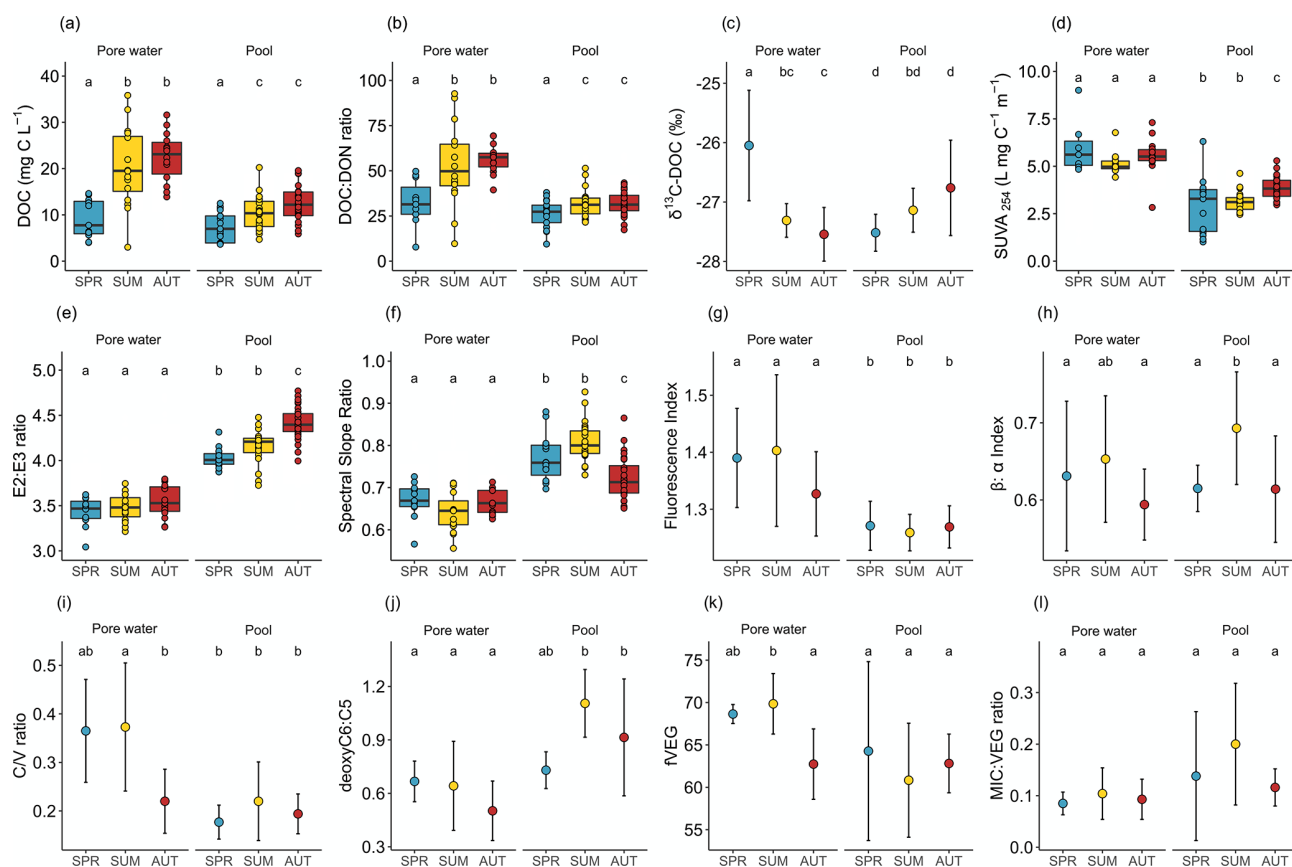


Figure 2. Box plots (a to b and d to f) and dot plots (c and g to i): (a) DOC concentrations, (b) DOC:DON ratio, (c) $\delta^{13}\text{C-DOC}$, (d) SUVA_{254} , (e) $E2:E3$ ratio, (f) spectral slope ratio, (g) fluorescence index, (h) $\beta:\alpha$ index, (i) C/V ratio, (j) deoxyC6:C5, (k) $f\text{VEG}$, and (l) MIC:VEG ratio. Each plot represents the evolution of variables during the growing season (SPR: spring; SUM: summer; AUT: autumn) in peat porewater and pools. Dot plots were used when $n < 5$ for at least one season. Error bars represent standard deviations. Box plots were used when $n > 5$ for each season. The dots represent each individual measurement, and boxes represent the lower (25th percentile) and the upper quartile (75th percentile); the median (50th percentile) is represented by the bold black horizontal bar in the boxes. Whiskers represent the interquartile range. Letters represent the significant differences between seasons. For each individual plot, conditions which share a letter do not present statistical differences.

pools, it decreased in peat porewater from 0.37 ± 0.12 during spring and summer to 0.22 ± 0.07 during autumn. Secondly, the deoxyC6:C5 ratio (Fig. 2j), a carbohydrate ratio, was significantly higher in pools (0.97 ± 0.28) than in peat porewater (0.57 ± 0.20) (p value < 0.0001). While it remained almost stable in peat porewater, it was maximal in summer (1.10 ± 0.19) compared to spring (0.73 ± 0.10) and autumn (0.91 ± 0.33). In pools, this evolution emphasized an increase in the contribution of microbial exudates among the carbohydrate compounds in pools. Finally, the fraction of plant-derived compounds among the identified markers, $f\text{VEG}$ (Fig. 2l), was always higher than 50% in both environments, highlighting the dominance of plant-derived DOM. However, $f\text{VEG}$ was significantly higher in peat porewater than in pools (p value = 0.02). Comparatively to the variations observed for the C/V ratio, $f\text{VEG}$ remained almost stable in pools, while it decreased in peat porewater in autumn.

4.6 Global assessment of DOM quality in peat porewaters and pools

The PCA analyses of the peat porewater and pool samples indicate that the first two components, represented by the two axes of Fig. 3, accounted for 56.3% of the total variance. Individuals represented in the first two dimensions showed a clear separation of both environments along the first dimension (Fig. 3). The major contributors of the first axis were S_R (19.8%), $E2:E3$ ratio (14.4%), deoxyC6:C5 (12.8%), DOC concentration (12.7%), and finally MIC:VEG ratio (11.8%). For the second axis, the major contributors were the proportion of phenols (%PHE-NOLS; 20.8%), C/V ratio (18.5%), and high-molecular-weight fatty acids (%HMW_FA; 17.3%). Other variables contributed less than 10% to the first two axes.

In pools, the DOM was characterized by a lower average molecular weight and aromaticity and a higher contri-

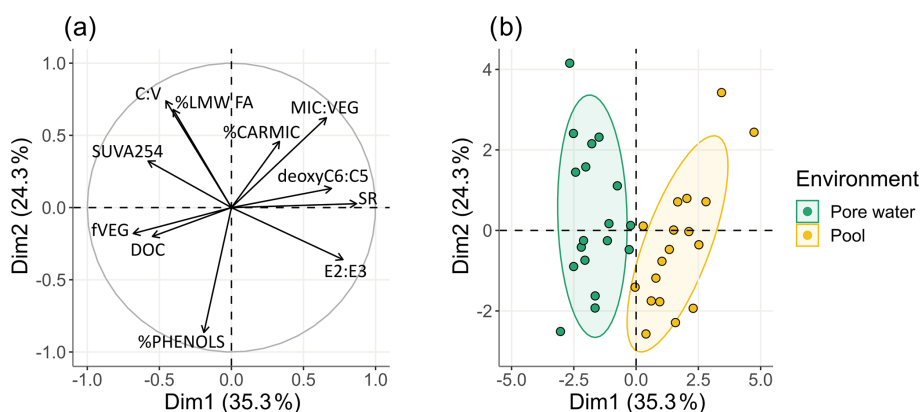


Figure 3. Representation of the first two dimensions of principal component analysis (PCA) of (a) physicochemical, quantitative, and qualitative parameters as variables and (b) individuals.

bution of microbial-derived DOM compared to peat porewater. Inversely, in peat porewater, the DOC concentrations were higher, and DOM presented higher aromaticity and a higher contribution of plant-derived DOM, characterized by a higher *f*VEG. There was no effect of the sampling season on the variances.

4.7 Experimental degradability of peat porewater and pool DOM

Statistical tests revealed no significant differences in the average degradation rate between in situ and controlled conditions of biodegradation (Sect. 3.5.1). In addition, no significant differences appeared between the average degradation rate where biodegradation only was tested and those where biodegradation and photodegradation were both tested. This suggests that temperature and sunlight had a limited effect on the DOM degradation. As a consequence, all experimental conditions (both in situ and controlled) were pooled in the following section. The DOM degradation rates were significantly higher for peat porewater than pools. The degradation rates were significantly higher for the incubation conditions of unfiltered samples (UF) compared to filtered sample (*F*) conditions (Fig. 4).

On average, the DOC degradation rates were 1.6 times higher for incubation under unfiltered conditions ($2.5 \pm 1.5 \text{ \% C d}^{-1}$) compared to filtered conditions ($1.5 \pm 0.8 \text{ \% C d}^{-1}$) in peat porewater. In pools, degradation rates were twice as high for UF ($1.1 \pm 1.1 \text{ \% C d}^{-1}$) than for *F* conditions ($0.5 \pm 0.6 \text{ \% C d}^{-1}$).

In peat porewater, the DOC degradation rates for *F* and UF conditions followed similar seasonal trends. The DOC degradation rates were low in June ($0.6 \pm 0.4 \text{ \% C d}^{-1}$) and twice as high for UF conditions ($1.3 \pm 1.0 \text{ \% C d}^{-1}$). The degradation rates reached a peak in August, with $2.2 \pm 0.5 \text{ \% C d}^{-1}$ for *F* and $4.5 \pm 0.8 \text{ \% C d}^{-1}$ for UF conditions. Then, the DOC degradation rates decreased in au-

tumn to $1.7 \pm 0.6 \text{ \% C d}^{-1}$ and $2.2 \pm 0.5 \text{ \% C d}^{-1}$ for *F* and UF incubation conditions, respectively.

After excluding the UF condition of August, there was no persistent significant difference between *F* and UF conditions. In June, the DOC degradation rates were similar between the *F* and UF conditions with rates of 1.0 ± 0.5 and $1.3 \pm 0.2 \text{ \% C d}^{-1}$, respectively. Then, an increase to $2.1 \pm 1.3 \text{ \% C d}^{-1}$ was observed in August for UF conditions which were 2 times lower than the rate measured in peat porewater under the same conditions. Finally, the DOC degradation rates diminished in September, with $0.8 \pm 0.3 \text{ \% C d}^{-1}$ for *F* and $1.1 \pm 0.3 \text{ \% C d}^{-1}$ for UF incubation conditions. Those degradation rates were 2 times lower than those observed in peat porewater in autumn.

As observed in Fig. 5, ΔSUVA_{254} was strongly and positively correlated with degradation rates, with specific dependence in pools ($n = 29$, $r = 0.82$; p value < 0.0001) and peat porewaters ($n = 33$, $r = 0.65$; p value < 0.0001).

5 Discussion

5.1 Differences in DOM concentrations and composition between peat porewaters and pools despite a similar source

The DOM concentration and composition strongly differed between peat porewater and pools, despite a clear common plant origin. Peat porewater DOM was characterized by high DOC concentrations and a DOM composed by both recently produced and biodegraded DOM. In pools, DOC concentrations were 2 times lower compared to the peat porewater (Fig. 2a). Pool DOM was characterized by a dominant contribution of allochthonous DOM (i.e., plant-derived) but also presented characteristics of microbial degraded DOM.

At our site located in the boreal ecozone, the average DOC concentration in peat porewater increased from 9.2 to 22.5 mg L^{-1} from spring to autumn. During the growing sea-

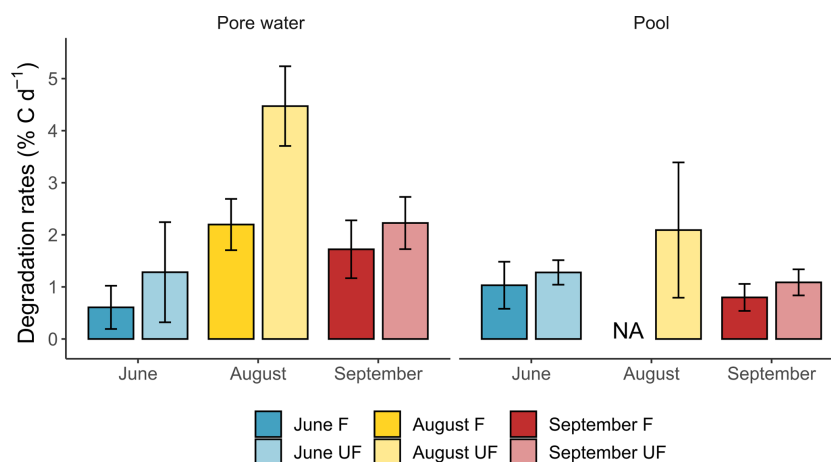


Figure 4. Seasonal degradation rates (in $\% \text{C d}^{-1}$) for DOC and TOC incubation conditions in peat porewater and pools.

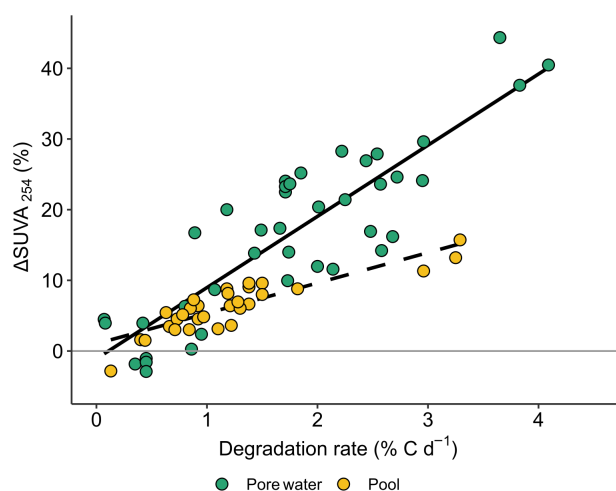


Figure 5. Relations between changes in SUVA_{254} (ΔSUVA_{254}) during incubation experiments and linear regression in peat porewater (solid line) and pools (dashed line).

son, DOC concentrations are in general below 20 mg L^{-1} in boreal and subarctic regions, which are lower than in temperate regions (Table S4). This latitudinal trend suggests that the balance between DOM production and processing in peat porewater is controlled by climate and most likely by temperature (Kane et al., 2014). At our site, both DOM production and consumption followed a strong seasonal trend in peat porewater, with DOM production being more intense, as DOC concentrations were multiplied by 2.5 during the growing season (Table 1).

DOM production by plants within peat porewater followed a strong seasonal trend. This is revealed by three observations. First, peat porewater showed a greater proportion of plant-derived DOM towards the end of the growing season as indicated by the lowest $\delta^{13}\text{C}$ -DOC measured in the autumn. Second, the high DOC: DON ratios measured in peat

porewater at our study site – up to 6 times higher than those measured in a temperate peatland by Austnes et al. (2010), as well as the DOC: DON ratio's increase along the growing season (Fig. 2b) – indicated a high contribution of recently produced DOM. Third, the slight decrease in $\delta^{13}\text{C}$ -DOC (Fig. 2c) and the contribution of high-molecular-weight fatty acids from spring to summer confirm the high contribution of plant-derived DOM. However, peat porewater DOM composition also suggested a contribution from microbial processing. First, the molecular analysis revealed the presence of microbial markers, as high as $6.4 \pm 2.7 \%$, as expressed by f_{MIC} (Table 1). Second, the incubation experiments highlighted that the labile fraction of DOM represented $2.0 \pm 1.3 \%$ of peat porewater DOC (Fig. 4). Third, the high SUVA_{254} values (Fig. 2d) we observed might reflect the importance of biodegradation processes of DOM in peat porewater as SUVA_{254} values increase with biodegradation (Hulatt et al., 2014; Autio et al., 2016, Fig. 5). The average SUVA_{254} of $5.5 \text{ L mg}^{-1} \text{ m}^{-1}$ measured in the Bouleau peatland porewater was, in general, higher than that previously measured in peatlands from temperate regions, i.e., $<3.6 \text{ L mg}^{-1} \text{ m}^{-1}$ (Arsenault et al., 2019; Tfaily et al., 2015; Heinz and Zak, 2018), except for Austnes et al. (2010), who reported a similar aromaticity and average DOM molecular weight in a Welsh ombrotrophic peatland. These indicators of microbial degradation within the peat also showed a seasonal trend, with higher DOM biodegradability measured in summer (Fig. 4), and the lowering of the f_{VEG} at the end of the growing season. Then, most of the DOM present in peat porewater is derived from the active vegetation at the surface of the peatland but has been partially decomposed through microbial degradation.

In pools, the DOM composition also presented specific features, with lower DOC concentrations, aromaticity, and average molecular weight compared to peat porewater (Fig. 2). Our results highlighted a dominant contribution of allochthonous DOM in pools despite the presence of

microbial-derived DOM. The DOC concentrations in pools (10.5 mg L^{-1} in average) were similar to those previously reported in the literature (Table S4), which, unlike peat porewater, do not follow any latitudinal trend. The DOC concentration remained relatively steady during the growing season, only multiplied by 1.6 compared to an increase by a factor of 2.5 in peat porewater (Table 1). The SUVA_{254} values measured in the Bouleau peatland pools ($3.4 \pm 0.9 \text{ L mg}^{-1} \text{ m}^{-1}$ on average; Fig. 2d) were similar to those reported from Arctic regions, with values of about $4 \text{ L mg}^{-1} \text{ m}^{-1}$ (Laurion and Mladenov, 2013; Peura et al., 2016; Gandois et al., 2019; Laurion et al., 2021), suggesting a contribution of plant-derived DOM from peat at our site and supported by the high DOC: DON ratio, ranging from 9.4 to 51.4 (Fig. 2b).

Yet, the slightly higher deoxyC6:C5 and the higher %LMW_FA in pools indicate the presence of microbial markers. Microbial processing follows a seasonal trend in pools (the highest microbial activity occurred in summer), which appear to be stronger compared to peat porewater. This is revealed by the evolution of $\delta^{13}\text{C}$ -DOC, increasing during the growing season (Fig. 2c) and revealing an increasing proportion of processed DOM. The increase in aromaticity, from 2.9 to 3.9 L cm^{-1} , might also reflect this microbial processing and its increasing contribution during the growing season. This is supported by indices as the S_R , deoxyC6:C5, MIC:VEG ratio, and β : α index following a pronounced seasonal trend with a peak reached in summer (Fig. 2). This suggests that pool DOM is mostly derived from active vegetation in the peat but undergoes more intense microbial degradation.

5.2 The DOM compositional differences between peat porewater and pools are explained by hydrological, chemical, and biological processes

The observed differences in DOM composition between peat porewater and pools were persistent during the growing season and under different hydroclimatic conditions. We propose that those differences were driven by a combination of hydrological, chemical, and biological factors. Along a peatland-to-pool transect, both DOM concentrations and compositions remained stable within the peatland and changed sharply at the interface between the peatland and an adjacent pool (Fig. S4).

Hydrological flow paths in the peatland and at the transitional zone between peat and pools might play a role in the shift of DOC concentrations and DOM composition between porewater and pools. The two environments appear to be hydrologically connected, based on synchronous variations of the water levels in adjacent environments with a strong buffering of water levels in pools (Fig. S2). This buffering can be explained by the decrease in hydraulic conductivity with depth in peat which limits water exchanges (Holden et al., 2018). This suggests that the preferential flow path for lateral advection occurs at shallower depths when WTD is

high (Birkel et al., 2017). Alternatively, it has been shown that deep flow paths (below 2 m depth) could supply surface flow (Levy et al., 2014; Peralta-Tapia et al., 2015), might transport deeper DOM to the surface water (Campeau et al., 2017), and could contribute to water supply in pools. The DOM composition in deep peat porewater has been reported to be relatively similar to shallow layers with high aromaticity and average molecular weight (Tfaily et al., 2018). If this process could provide DOM to pools, it could not explain the shift in DOM composition between environments.

At our studied peatland, a decrease in the water storage coefficient (Riahi et al., submitted) and an increase in peat density with depth has been documented (Primeau and Garneau, 2021), which should inhibit water flow movements. In addition to slower water circulation, peat pore structure stimulates interactions between DOM and partially degraded peat, which can adsorb both hydrophilic and hydrophobic compounds (Kalbitz et al., 2000; Rezanezhad et al., 2016). Changes in composition between peat porewater and pools might be induced by the selective interaction between DOM aromatic compounds and peat during their slow transfer. As we observed SUVA_{254} values 1.6 times higher in peat porewater compared to pools (Fig. 2), those aromatic products might selectively interact with peat or at least reduce its mobility and explain the lower DOC concentration and DOM aromaticity measured in pools (Table 1), since aromatic compounds are known to constitute the hydrophobic fraction of DOM (Dilling and Kaiser, 2002).

Then, DOM microbial processing, occurring at different rates within peat, at the interface between peat and pools and within the pool, might greatly contribute to the observed differences in DOM composition. Peat porewater DOM composition reflects microbial degradation occurring within the peat (f_{MIC} , Table 1) and shows a greater degradation potential compared to pool DOM (Fig. 4). The slow water circulation and long residence time of DOM within peat might promote interactions with microorganisms, allowing microbial degradation of DOM (Kalbitz et al., 2000; Catalán et al., 2016). Yet, a significantly higher contribution of microbial-derived DOM was observed in pools, as expressed by a higher deoxyC6:C5 and higher %LMW_FA and lower f_{VEG} indices, as well as the decrease in the average DOM molecular weight as shown by the higher S_R and E2:E3 ratio. The significantly lower C/V ratio measured in pools also supports the higher DOM microbial processing in pools. The coumaric and ferulic acids, composing the C fraction, are preferentially biodegraded compared the vanillic acid, vanillin, and acetovanillone, composing the V fraction (Goñi and Hedges, 1992), resulting in a decrease in the C/V ratio, as observed from peat porewater to pools.

The signature of microbial-derived DOM in pools supports the hypothesis that DOM degradation processes occur at the interface between peat porewater and pools (Fig. S4) and within the pools. A shift gradual sharp changes in physicochemical parameters between the two environments, such

as the slight increase in pH and temperature, and the rise of dissolved oxygen concentrations may favor the microbial turnover of the fraction of labile peat porewater DOM (higher than in pool, Fig. 4; Schindler et al., 1997; Kalbitz et al., 2000; Worrall et al., 2008; Peura et al., 2016). Additionally, our data did not evidence any photodegradation during DOM incubation in peat porewater and pools, suggesting that the DOM photodegradation was not sizable by our experimental design. This contrasts with previous studies which observed DOM photodegradation and changes in DOM composition in boreal and temperate aquatic ecosystems of eastern Canada (Lapierre and del Giorgio, 2014; Ward and Cory, 2016) and the United Kingdom (Jones et al., 2016). The absence of sizable photodegradation suggests that this process did not drive the DOM composition in pools, compared to biodegradation. The clear pattern of the SUVA₂₅₄ increase observed during the incubation experiments was independent to the exposition of DOM with the solar radiation. This is consistent with the biodegradation of non-aromatic molecules (Spencer et al., 2008, 2015; Mann et al., 2015; Worrall et al., 2017), leading to an increase in SUVA₂₅₄ (Hulatt et al., 2014; Autio et al., 2016), while photooxidation has been shown to induce a decrease in DOM aromaticity (Laurion and Mladenov, 2013; Ward and Cory, 2016). This supports the hypothesis that the peat-derived DOM biodegradation is an important driver of DOM composition in the pools.

5.3 Implications of the DOM exchange from peat to pools for the peatland carbon cycle

Boreal peatland pools were previously identified as a continuous source of carbon dioxide (CO₂) to the atmosphere during ice-free seasons, offsetting some of the carbon uptake by the vegetation (Pelletier et al., 2014, 2015). This release of CO₂ was assumed to be the product of DOM mineralization through microbial productivity in pools (Billett et al., 2004; Striegl et al., 2012; Payandi-Rolland et al., 2020). Since our results showed low degradation rates in pools, we suggest that DOM could have been partially biodegraded within the peat and at the interface zone between peat porewater and pools, limiting further its degradation within pools (Payandi-Rolland et al., 2020). This reactive interface could be comparable with the hyporheic zone (riparian-water-saturated zone between the peat and the stream), which can be an active component of the carbon cycle through the active DOM mineralization and CH₄ oxidation at this interface (Rasilo et al., 2017).

The long-term apparent rate of carbon accumulation (LORCA) measured in the Bouleau peatland has been estimated to be 35.5 g C m⁻² yr⁻¹ and the recent apparent rate of carbon accumulation (RERCA) 85.1 g C m⁻² yr⁻¹ (Primeau and Garneau, 2021). Based on a total pool volume of approximately 136 350 m³, an average DOC concentration of 10.1 mg L⁻¹ (Table 1), and an average potential degradation rate between 1.9 % d⁻¹ in peat porewater and 0.9 % d⁻¹ in

pools (Fig. 4), the degradation of pool DOM could average between 1.5 and 3.1 g C m⁻² y⁻¹ for our site. This is equivalent to 5.4 % to 11.1 % of the LORCA and 2.2 % to 4.6 % of the RERCA. Those proportions suggest that the processing of DOM in pools might have a substantial impact on the peatland carbon budget. The integration of carbon exchange at the pool–atmosphere interface would tend to ultimately minimize the carbon sink capacity of peatlands often reported from studies focusing on vegetation-to-atmosphere exchange. It is also important to note that DOM in pools is mainly derived from the recently produced DOM in peat, is unlikely from deeper (and older) peat layers, and might not affect old carbon stocks from deeper peat horizons. However, DOM degradation is not the only source of carbon emissions from pools which can also be supplied by the lateral transfer of CO₂ and CH₄ (Rasilo et al., 2017) and by CH₄ ebullition (Repo et al., 2007). However, the importance of the pools as a potential carbon source to the atmosphere needs to be moderate in comparison with the CO₂ and the CH₄ exported and emitted in the headwater stream of the peatland. This flux of 8.8 g C m⁻² yr⁻¹ (Taillardat et al., 2022) accounted for 22.8 % of the LORCA, which is between 2 and 4 times higher than the carbon potentially emitted by pools.

Results presented in this study are from a boreal peatland, without permafrost or anthropogenic disturbances that could influence the carbon production and transformation processes through the peat–pool complex. The morphology of pool banks and vegetation surrounding the pools may play an important role in the DOM dynamics and DOC concentrations of pools, as suggested by Arsenault et al. (2018, 2019), who studied 156 pools with a range of surface and depth comparable to our study site. A study conducted on 10 peatland pools showed that the size of the contact surface between water and peat (influenced by pool size, depth, and the slope of the banks) influenced the concentrations and composition of DOM (Ban e, 2013). However, the pools studied by Ban e (2013) were up to 10 times larger and deeper than in our studied peatland pools. At our site, there was no significant difference between the pools in their range of size (from 30 to 2065 m²) and depth (from 70 to 120 cm) except for SUVA₂₅₄ (Table S5). Despite the slight effect observed on SUVA₂₅₄, the DOM dynamics do not seem related to the pool morphology and depth. It supports the hypothesis that DOM transfer and biodegradation from peat porewater to pools are the main driver of its dynamic and implication to the peatland carbon cycle rather than pool morphological features.

Our study suggests that peat-derived DOM degradation and release through pools could play a substantial role on the net carbon budget of our studied peatland (<10 % of the LORCA). Moreover, the influence of pools in the peatland carbon cycle should be considered from the perspective of climate change. DOM production and biodegradation rates seem to be controlled by temperature (Figs. 2 and 4) during the growing season, and longer ice-free seasons and higher

temperatures might impact the importance of pools in the peatland carbon cycle.

6 Conclusion

This study demonstrated that DOM is a highly dynamic component of the carbon cycle in peatland, with important differences identified in its concentration and composition in both peat porewater and pools. Those differences are persistent throughout the growing season and different hydroclimatic conditions.

The strong increase in DOC concentrations in peat porewater over the growing season highlighted the intense production of DOM in this environment. DOC concentrations increased by 2.5 during the growing season (against a DOC concentration increase by a factor of 1.7 of in pools), despite microbial processing of DOM occurring within the peat.

The molecular analysis of DOM in pools revealed the dominant contribution of allochthonous DOM derived from the peatland vegetation, supported by the dominance of plant makers (f_{VEG} and %Phenols) and high DOC : DON ratio. Despite this similar plant origin, peat porewater and pools DOM had very different concentrations, composition, and dynamics over the growing season. The DOM in pools was less aromatic and showed lower molecular weight compared to peat porewater.

Based on our investigations, we suggest that a combination of hydrological, chemical, and biological processes explain those differences. The low hydraulic conductivity in peat might favor DOM microbial processing before its transfer to the aquatic compartments. Low hydraulic conductivity could also lead to the selective adsorption of aromatic compounds with degraded peat supporting the decrease in concentration and the lower aromaticity of DOM observed in pools. We observed abrupt changes in DOM concentration and composition at the interface between peat and pools which were persistent during the growing season. The rapid modification of physicochemical conditions (e.g., temperature and oxygen availability) between those two environments might influence the biodegradation of DOM at the interface between the peat and the pools and within the pools. This is confirmed by the higher proportion of microbial molecular markers identified in the pool.

Although DOM is microbially degraded both at the interface and within the pool, the carbon emissions generated by those processes could be substantial (between 5.5 % and 11 % of the LORCA). The importance of pools in the carbon cycle still needs to be studied in the context of increasing temperatures, which could stimulate DOM production in peat porewater and its microbial processing in peat porewater, as well as in pools after its transfer.

Data availability. The data sets used in this study are available online on the PANGAEA data repository (<https://doi.org/10.1594/PANGAEA.945391>, Prijac et al., 2022).

Supplement. The supplement related to this article is available online at: <https://doi.org/10.5194/bg-19-4571-2022-supplement>.

Author contributions. LG, MG, AP, and PT carried out the conceptualization. AP performed the data curation with input from LJ and PT, as well as the data analyses with input from LJ. LG and AP performed the formal analyses. MG was responsible for the funding acquisition. LG, LJ, and AP developed the methodology. AP and PT performed the data collection with the help of LG and MG. AP wrote the original draft and developed the figures. All coauthors contributed to the review and editing.

Competing interests. The contact author has declared that none of the authors has any competing interests.

Disclaimer. Publisher's note: Copernicus Publications remains neutral with regard to jurisdictional claims in published maps and institutional affiliations.

Acknowledgements. We thank Katherine Velghe and Alice Parks from GRIL for their laboratory training and assistance in absorbance and fluorescence analyses, as well as Paul Del Giorgio for access to his laboratory. Marine Liotaud, from Géosciences Rennes, is acknowledged for performing THM-GC-MS analyses, and Frédéric Julien, Virginie Payre-Suc, and Didier Lambrigtot, from Laboratoire Ecologie Fonctionnelle et Environnement, are acknowledged for performing DOC/TN and cations/anions analyses. We thank Roman Teisserenc (Ensat, Toulouse) and Charles Bonneau, Charles-Élie Dubé-Poirier, Camille Girard, Pénélope Germain-Chartrand, Léonie Perrier, Guillaume Primeau, Khawla Riahi, and Karelle Trottier for their assistance in the field.

Financial support. This research has been supported by the Natural Sciences and Engineering Research Council of Canada and Hydro-Québec funding to Michelle Garneau (grant no. RDCPJ 51421817).

Review statement. This paper was edited by Gwenaél Abril and reviewed by Audrey Campeau and one anonymous referee.

References

Arsenault, J., Talbot, J., and Moore, T. R.: Environmental controls of C, N and P biogeochemistry in peatland pools, *Sci. Total Environ.*, 631–632, 714–722, <https://doi.org/10.1016/j.scitotenv.2018.03.064>, 2018.

- Arsenault, J., Talbot, J., Moore, T. R., Beauvais, M., Franssen, J., and Roulet, N. T.: The Spatial Heterogeneity of Vegetation, Hydrology and Water Chemistry in a Peatland with Open-Water Pools, *Ecosystems*, 22, 1352–1367, <https://doi.org/10.1007/s10021-019-00342-4>, 2019.
- Austnes, K., Evans, C. D., Eliot-Laize, C., Naden, P. S., and Old, G. H.: Effects of storm events on mobilisation and in-stream processing of dissolved organic matter (DOM) in a Welsh peatland catchment, *Biogeochemistry*, 99, 157–173, <https://doi.org/10.1007/s10533-009-9399-4>, 2010.
- Autio, I., Soinne, H., Helin, J., Asmala, E., and Hoikkala, L.: Effect of catchment land use and soil type on the concentration, quality, and bacterial degradation of riverine dissolved organic matter, *Ambio*, 45, 331–349, <https://doi.org/10.1007/s13280-015-0724-y>, 2016.
- Banaś, K.: The hydrochemistry of peatland lakes as a result of the morphological characteristics of their basins, *Oceanol. Hydrobiol. Stud.*, 42, 28–39, <https://doi.org/10.2478/s13545-013-0057-z>, 2013.
- Billett, M. F., Palmer, S. M., Hope, D., Deacon, C., Storeton-West, R., Hargreaves, K. J., Flechar, C., and Fowler, D.: Linking land-atmosphere-stream carbon fluxes in a lowland peatland system, *Global Biogeochem. Cy.*, 18, GB1024, <https://doi.org/10.1029/2003GB002058>, 2004.
- Billett, M. F., Deacon, C. M., Palmer, S. M., Dawson, J. J. C., and Hope, D.: Connecting organic carbon in stream water and soils in a peatland catchment, *J. Geophys. Res. Biogeo.*, 111, G02010, <https://doi.org/10.1029/2005JG000065>, 2006.
- Billett, M. F., Dinsmore, K. J., Smart, R. P., Garnett, M. H., Holden, J., Chapman, P., Baird, A. J., Grayson, R., and Stott, A. W.: Variable source and age of different forms of carbon released from natural peatland pipes, *J. Geophys. Res. Biogeo.*, 117, G02003, <https://doi.org/10.1029/2011JG001807>, 2012.
- Birkel, C., Broder, T., and Biester, H.: Nonlinear and threshold-dominated runoff generation controls DOC export in a small peat catchment, *J. Geophys. Res. Biogeo.*, 122, 498–513, <https://doi.org/10.1002/2016JG003621>, 2017.
- Blodau, C., Roulet, N. T., Heitmann, T., Stewart, H., Beer, J., Lafleur, P., and Moore, T. R.: Belowground carbon turnover in a temperate ombrotrophic bog: BELOWGROUND C TURNOVER, *Global Biogeochem. Cy.*, 21, GB1021, <https://doi.org/10.1029/2005GB002659>, 2007.
- Burd, K., Estop-Aragonés, C., Tank, S. E., and Olefeldt, D.: Lability of dissolved organic carbon from boreal peatlands: interactions between permafrost thaw, wildfire, and season, *Can. J. Soil Sci.*, 100, 503–515, <https://doi.org/10.1139/cjss-2019-0154>, 2020.
- Buzek, F., Novak, M., Cejkova, B., Jackova, I., Curik, J., Veselovsky, F., Stepanova, M., Prechova, E., and Bohdalkova, L.: Assessing DOC export from a *Sphagnum*-dominated peatland using $\delta^{13}\text{C}$ and $\delta^{18}\text{O}$ - H_2O stable isotopes, *Hydrol. Process.*, 33, 2792–2803, <https://doi.org/10.1002/hyp.13528>, 2019.
- Campeau, A., Bishop, K. H., Billett, M. F., Garnett, M. H., Laudon, H., Leach, J. A., Nilsson, M. B., Öquist, M. G., and Wallin, M. B.: Aquatic export of young dissolved and gaseous carbon from a pristine boreal fen: Implications for peat carbon stock stability, *Glob. Change Biol.*, 23, 5523–5536, <https://doi.org/10.1111/gcb.13815>, 2017.
- Catalán, N., Marcé, R., Kothawala, D. N., and Tranvik, Lars. J.: Organic carbon decomposition rates controlled by water retention time across inland waters, *Nat. Geosci.*, 9, 501–504, <https://doi.org/10.1038/ngeo2720>, 2016.
- Charman, D.: *Peatlands and Environment Change*, 1st edn., Wiley, 320 pp., ISBN:978-0-470-84410-6, 2002.
- Chaudhary, N., Miller, P. A., and Smith, B.: Biotic and Abiotic Drivers of Peatland Growth and Microtopography: A Model Demonstration, *Ecosystems*, 21, 1196–1214, <https://doi.org/10.1007/s10021-017-0213-1>, 2018.
- Cory, R. M., Miller, M. P., McKnight, D. M., Guerard, J. J., and Miller, P. L.: Effect of instrument-specific response on the analysis of fulvic acid fluorescence spectra: Evaluating instrument-specific response, *Limnol. Oceanogr. Methods*, 8, 67–78, <https://doi.org/10.4319/lom.2010.8.67>, 2010.
- Dean, J. F., Garnett, M. H., Spyarakos, E., and Billett, M. F.: The Potential Hidden Age of Dissolved Organic Carbon Exported by Peatland Streams, *J. Geophys. Res.*, 124, 328–341, <https://doi.org/10.1029/2018JG004650>, 2019.
- Deshpande, B. N., Crevecoeur, S., Matveev, A., and Vincent, W. F.: Bacterial production in subarctic peatland lakes enriched by thawing permafrost, *Biogeosciences*, 13, 4411–4427, <https://doi.org/10.5194/bg-13-4411-2016>, 2016.
- Dilling, J. and Kaiser, K.: Estimation of the hydrophobic fraction of dissolved organic matter in water samples using UV photometry, *Water Res.*, 36, 5037–5044, [https://doi.org/10.1016/S0043-1354\(02\)00365-2](https://doi.org/10.1016/S0043-1354(02)00365-2), 2002.
- Dubois, J. M. M.: Environnements quaternaires et évolution postglaciaire d'une zone côtière en émergence en bordure sud du bouclier canadien: la moyenne Côte Nord du Saint-Laurent, Québec, University of Ottawa, Ottawa, <https://doi.org/10.20381/ruor-15610>, 1980.
- Elder, J. F., Rybicki, N. B., Carter, V., and Weintraub, V.: Sources and yields of dissolved carbon in northern Wisconsin stream catchments with differing amounts of peatland, *Wetlands*, 20, 113–125, [https://doi.org/10.1672/0277-5212\(2000\)020\[0113:SAYODC\]2.0.CO;2](https://doi.org/10.1672/0277-5212(2000)020[0113:SAYODC]2.0.CO;2), 2000.
- Folhas, D., Duarte, A. C., Pilote, M., Vincent, W. F., Freitas, P., Vieira, G., Silva, A. M. S., Duarte, R. M. B. O., and Canário, J.: Structural Characterization of Dissolved Organic Matter in Permafrost Peatland Lakes, *Water*, 12, 3059, <https://doi.org/10.3390/w12113059>, 2020.
- Frey, K. E., Sobczak, W. V., Mann, P. J., and Holmes, R. M.: Optical properties and bioavailability of dissolved organic matter along a flow-path continuum from soil pore waters to the Kolyma River mainstem, East Siberia, *Biogeosciences*, 13, 2279–2290, <https://doi.org/10.5194/bg-13-2279-2016>, 2016.
- Gandois, L., Hoyt, A. M., Hatté, C., Jeanneau, L., Teisserenc, R., Liotaud, M., and Tananaev, N.: Contribution of Peatland Permafrost to Dissolved Organic Matter along a Thaw Gradient in North Siberia, *Environ. Sci. Technol.*, 53, 14165–14174, <https://doi.org/10.1021/acs.est.9b03735>, 2019.
- Goñi, M. A. and Hedges, J. I.: Lignin dimers: Structures, distribution, and potential geochemical applications, *Geochim. Cosmochim. Ac.*, 56, 4025–4043, [https://doi.org/10.1016/0016-7037\(92\)90014-A](https://doi.org/10.1016/0016-7037(92)90014-A), 1992.
- Graham, J. D., Glenn, N. F., Spaete, L. P., and Hanson, P. J.: Characterizing Peatland Microtopography Using Gradient and Microform-Based Approaches, *Ecosystems*, 23, 1464–1480, <https://doi.org/10.1007/s10021-020-00481-z>, 2020.

- Haan, H. D. and Boer, T. D.: Applicability of light absorbance and fluorescence as measures of concentration and molecular size of dissolved organic carbon in humic Lake Tjeukemeer, *Water Res.*, 21, 731–734, [https://doi.org/10.1016/0043-1354\(87\)90086-8](https://doi.org/10.1016/0043-1354(87)90086-8), 1987.
- Heinz, M. and Zak, D.: Storage effects on quantity and composition of dissolved organic carbon and nitrogen of lake water, leaf leachate and peat soil water, *Water Res.*, 130, 98–104, <https://doi.org/10.1016/j.watres.2017.11.053>, 2018.
- Helms, J. R., Stubbins, A., Ritchie, J. D., Minor, E. C., Kieber, D. J., and Mopper, K.: Absorption spectral slopes and slope ratios as indicators of molecular weight, source, and photobleaching of chromophoric dissolved organic matter, *Limnol. Oceanogr.*, 53, 955–969, <https://doi.org/10.4319/lo.2008.53.3.0955>, 2008.
- Holden, J., Moody, C. S., Edward Turner, T., McKenzie, R., Baird, A. J., Billett, M. F., Chapman, P. J., Dinsmore, K. J., Grayson, R. P., Andersen, R., Gee, C., and Dooling, G.: Water-level dynamics in natural and artificial pools in blanket peatlands, *Hydrol. Process.*, 32, 550–561, <https://doi.org/10.1002/hyp.11438>, 2018.
- Hulatt, C. J., Kaartokallio, H., Asmala, E., Autio, R., Stedmon, C. A., Sonninen, E., Oinonen, M., and Thomas, D. N.: Bioavailability and radiocarbon age of fluvial dissolved organic matter (DOM) from a northern peatland-dominated catchment: effect of land-use change, *Aquat. Sci.*, 76, 393–404, <https://doi.org/10.1007/s00027-014-0342-y>, 2014.
- Jaffé, R., Yamashita, Y., Maie, N., Cooper, W. T., Dittmar, T., Dodds, W. K., Jones, J. B., Myoshi, T., Ortiz-Zayas, J. R., Podgorski, D. C., and Watanabe, A.: Dissolved Organic Matter in Headwater Streams: Compositional Variability across Climatic Regions of North America, *Geochim. Cosmochim. Ac.*, 94, 95–108, <https://doi.org/10.1016/j.gca.2012.06.031>, 2012.
- Jeanneau, L., Jaffrezic, A., Pierson-Wickmann, A.-C., Gruau, G., Lambert, T., and Petitjean, P.: Constraints on the Sources and Production Mechanisms of Dissolved Organic Matter in Soils from Molecular Biomarkers, *Vadose Zone J.*, 13, vjz2014.02.0015, <https://doi.org/10.2136/vjz2014.02.0015>, 2014.
- Jeanneau, L., Denis, M., Pierson-Wickmann, A.-C., Gruau, G., Lambert, T., and Petitjean, P.: Sources of dissolved organic matter during storm and inter-storm conditions in a lowland headwater catchment: constraints from high-frequency molecular data, *Biogeosciences*, 12, 4333–4343, <https://doi.org/10.5194/bg-12-4333-2015>, 2015.
- Jones, T. G., Evans, C. D., Jones, D. L., Hill, P. W., and Freeman, C.: Transformations in DOC along a source to sea continuum: impacts of photo-degradation, biological processes and mixing, *Aquat. Sci.*, 78, 433–446, <https://doi.org/10.1007/s00027-015-0461-0>, 2016.
- Kaal, J., Cortizas, A. M., and Biester, H.: Downstream changes in molecular composition of DOM along a headwater stream in the Harz mountains (Central Germany) as determined by FTIR, Pyrolysis-GC-MS and THM-GC-MS, *J. Anal. Appl. Pyrolysis*, 126, 50–61, <https://doi.org/10.1016/j.jaap.2017.06.025>, 2017.
- Kaal, J., Plaza, C., Nierop, K. G. J., Pérez-Rodríguez, M., and Biester, H.: Origin of dissolved organic matter in the Harz Mountains (Germany): A thermally assisted hydrolysis and methylation (THM-GC-MS) study, *Geoderma*, 378, 114635, <https://doi.org/10.1016/j.geoderma.2020.114635>, 2020.
- Kalbitz, K., Solinger, S., Park, J.-H., Michalzik, B., and Matzner, E.: Controls On The Dynamics Of Dissolved Organic Matter In Soils: A Review, *Soil Sci.*, 165, 277–304, <https://doi.org/10.1097/00010694-200004000-00001>, 2000.
- Kane, E. S., Mazzoleni, L. R., Kratz, C. J., Hribljan, J. A., Johnson, C. P., Pypker, T. G., and Chimner, R.: Peat porewater dissolved organic carbon concentration and lability increase with warming: a field temperature manipulation experiment in a poor-fen, *Biogeochemistry*, 119, 161–178, <https://doi.org/10.1007/s10533-014-9955-4>, 2014.
- Kaplan, L. A. and Cory, R. M.: Dissolved Organic Matter in Stream Ecosystems, in: *Stream Ecosystems in a Changing Environment*, Elsevier, 241–320, <https://doi.org/10.1016/B978-0-12-405890-3.00006-3>, 2016.
- Knorr, K.-H.: DOC-dynamics in a small headwater catchment as driven by redox fluctuations and hydrological flow paths – are DOC exports mediated by iron reduction/oxidation cycles?, *Biogeosciences*, 10, 891–904, <https://doi.org/10.5194/bg-10-891-2013>, 2013.
- Lalonde, K., Middlestead, P., and Gélinas, Y.: Automation of $^{13}\text{C}/^{12}\text{C}$ ratio measurement for freshwater and seawater DOC using high temperature combustion, *Limnol. Oceanogr. Methods*, 12, 816–829, <https://doi.org/10.4319/lom.2014.12.816>, 2014.
- Lapierre, J.-F. and del Giorgio, P. A.: Partial coupling and differential regulation of biologically and photochemically labile dissolved organic carbon across boreal aquatic networks, *Biogeosciences*, 11, 5969–5985, <https://doi.org/10.5194/bg-11-5969-2014>, 2014.
- Laurion, I. and Mladenov, N.: Dissolved organic matter photolysis in Canadian arctic thaw ponds, *Environ. Res. Lett.*, 8, 035026, <https://doi.org/10.1088/1748-9326/8/3/035026>, 2013.
- Laurion, I., Massicotte, P., Mazoyer, F., Negandhi, K., and Mladenov, N.: Weak mineralization despite strong processing of dissolved organic matter in Eastern Arctic tundra ponds, *Limnol. Oceanogr.*, 66, 1–17, <https://doi.org/10.1002/lno.11634>, 2021.
- Lê, S., Josse, J., and Husson, F.: FactoMineR: An R Package for Multivariate Analysis, *J. Stat. Softw.*, 25, 1–18, <https://doi.org/10.18637/jss.v025.i01>, 2008.
- Levy, Z. F., Siegel, D. I., Dasgupta, S. S., Glaser, P. H., and Welker, J. M.: Stable isotopes of water show deep seasonal recharge in northern bogs and fens, *Hydrol. Process.*, 28, 4938–4952, <https://doi.org/10.1002/hyp.9983>, 2014.
- Mann, P. J., Eglinton, T. I., McIntyre, C. P., Zimov, N., Davydova, A., Vonk, J. E., Holmes, R. M., and Spencer, R. G. M.: Utilization of ancient permafrost carbon in headwaters of Arctic fluvial networks, *Nat. Commun.*, 6, 7856, <https://doi.org/10.1038/ncomms8856>, 2015.
- McKnight, D. M., Andrews, E. D., Spaulding, S. A., and Aiken, G. R.: Aquatic fulvic acids in algal-rich antarctic ponds, *Limnol. Oceanogr.*, 39, 1972–1979, <https://doi.org/10.4319/lo.1994.39.8.1972>, 1994.
- McKnight, D. M., Boyer, E. W., Westerhoff, P. K., Doran, P. T., Kulbe, T., and Andersen, D. T.: Spectrofluorometric characterization of dissolved organic matter for indication of precursor organic material and aromaticity, *Limnol. Oceanogr.*, 46, 38–48, <https://doi.org/10.4319/lo.2001.46.1.0038>, 2001.
- Meteorological Service of Canada and Environment and Climate Change Canada: Historical daily weather data from the station

- Havre Saint Pierre A (1990–2019), Meteorological Service of Canada and Environment and Climate Change Canada [data set], <https://climatedata.ca/download/#station-download> (last access: 18 September 2022), 2019.
- Moody, C. S. and Worrall, F.: Towards understanding organic matter fluxes and reactivity in surface waters: Filtering impact on DOC / POC degradation, *Hydrol. Process.*, 35, e14067, <https://doi.org/10.1002/hyp.14067>, 2021.
- Nungesser, M. K.: Modelling microtopography in boreal peatlands: hummocks and hollows, *Ecol. Model.*, 165, 175–207, [https://doi.org/10.1016/S0304-3800\(03\)00067-X](https://doi.org/10.1016/S0304-3800(03)00067-X), 2003.
- Parlanti, E.: Dissolved organic matter fluorescence spectroscopy as a tool to estimate biological activity in a coastal zone submitted to anthropogenic inputs, *Org. Geochem.*, 31, 1765–1781, 2000.
- Payandi-Rolland, D., Shirokova, L. S., Tesfa, M., Bénétheth, P., Lim, A. G., Kuzmina, D., Karlsson, J., Giesler, R., and Pokrovsky, O. S.: Dissolved organic matter biodegradation along a hydrological continuum in permafrost peatlands, *Sci. Total Environ.*, 749, 141463, <https://doi.org/10.1016/j.scitotenv.2020.141463>, 2020.
- Payette, S.: Le contexte physique et biogéographique., in: *Écologie des tourbières du Québec-Labrador*, edited by: Payette, S. and Rochefort, L., Presses de l'Université Laval, Québec, 9–37, ISBN: 9782763777733, 2001.
- Pelletier, L., Garneau, M., and Moore, T. R.: Variation in CO₂ exchange over three summers at microform scale in a boreal bog, Eastmain region, Québec, Canada, *J. Geophys. Res.*, 116, G03019, <https://doi.org/10.1029/2011JG001657>, 2011.
- Pelletier, L., Strachan, I. B., Garneau, M., and Roulet, N. T.: Carbon release from boreal peatland open water pools: Implication for the contemporary C exchange: Carbon release from peatland pools, *J. Geophys. Res. Biogeo.*, 119, 207–222, <https://doi.org/10.1002/2013JG002423>, 2014.
- Pelletier, L., Strachan, I. B., Roulet, N. T., and Garneau, M.: Can boreal peatlands with pools be net sinks for CO₂?, *Environ. Res. Lett.*, 10, 035002, <https://doi.org/10.1088/1748-9326/10/3/035002>, 2015.
- Peralta-Tapia, A., Sponseller, R. A., Tetzlaff, D., Soulsby, C., and Laudon, H.: Connecting precipitation inputs and soil flow pathways to stream water in contrasting boreal catchments, *Hydrol. Process.*, 29, 3546–3555, <https://doi.org/10.1002/hyp.10300>, 2015.
- Peura, S., Wauthy, M., Simone, D., Eiler, A., Einarsdóttir, K., Rautio, M., and Bertilsson, S.: Ontogenic succession of thermokarst thaw ponds is linked to dissolved organic matter quality and microbial degradation potential, *Limnol. Oceanogr.*, 65, S248–S263, <https://doi.org/10.1002/lno.11349>, 2016.
- Prijac, A., Gandois, L., Jeanneau, L., Taillardat, P., and Garneau, M.: Concentration, composition and potential degradation of dissolved organic matter derived from peat porewater and pools discrete sampling of an ombrotrophic boreal peatland (Minganie, Québec, Canada), PANGAEA [data set], <https://doi.org/10.1594/PANGAEA.945391>, 2022.
- Primeau, G. and Garneau, M.: Carbon accumulation in peatlands along a boreal to subarctic transect in eastern Canada, *The Holocene*, 31, 858–869, <https://doi.org/10.1177/0959683620988031>, 2021.
- Rasilo, T., Hutchins, R. H. S., Ruiz-González, C., and del Giorgio, P. A.: Transport and transformation of soil-derived CO₂, CH₄ and DOC sustain CO₂ supersaturation in small boreal streams, *Sci. Total Environ.*, 579, 902–912, <https://doi.org/10.1016/j.scitotenv.2016.10.187>, 2017.
- Raymond, P. A. and Spencer, R. G. M.: Riverine DOM, in: *Biogeochemistry of Marine Dissolved Organic Matter*, edited by: Hansell, D. A. and Carlson, C. A., Elsevier, 509–533, <https://doi.org/10.1016/B978-0-12-405940-5.00011-X>, 2015.
- Repo, E., Huttunen, J. T., Naumov, A. V., Chichulin, A. V., Lapshina, E. D., Bleuten, W., and Martikainen, P. J.: Release of CO₂ and CH₄ from small wetland lakes in western Siberia, *Tellus B*, 59, 788–796, <https://doi.org/10.1111/j.1600-0889.2007.00301.x>, 2007.
- Rezanezhad, F., Price, J. S., Quinton, W. L., Lennartz, B., Milojevic, T., and Cappellen, P. V.: Structure of peat soils and implications for water storage, flow and solute transport: A review update for geochemists, *Chem. Geol.*, 10, 75–84, <https://doi.org/10.1016/j.chemgeo.2016.03.010>, 2016.
- Rosset, T., Gandois, L., Le Roux, G., Teisserenc, R., Duran-tes Jimenez, P., Camboulive, T., and Binet, S.: Peatland Contribution to Stream Organic Carbon Exports From a Montane Watershed, *J. Geophys. Res. Biogeo.*, 124, 3448–3464, <https://doi.org/10.1029/2019JG005142>, 2019.
- Rumpel, C. and Dignac, M.-F.: Gas chromatographic analysis of monosaccharides in a forest soil profile: Analysis by gas chromatography after trifluoroacetic acid hydrolysis and reduction–acetylation, *Soil Biol. Biochem.*, 38, 1478–1481, <https://doi.org/10.1016/j.soilbio.2005.09.017>, 2006.
- Rydin, H., Jeglum, J. K., and Bennett, K. D.: *The biology of peatlands*, 2nd edn., Oxford University Press, Oxford, 382 pp., ISBN: 9780199603008, 2013.
- Schindler, D. W., Curtis, P. J., Bayley, S. E., Parker, B. R., Beaty, K. G., and Stainton, M. P.: Climate-induced changes in the dissolved organic carbon budgets of boreal lakes, *Biogeochemistry*, 36, 9–28, 1997.
- Shi, X., Thornton, P. E., Ricciuto, D. M., Hanson, P. J., Mao, J., Sebestyen, S. D., Griffiths, N. A., and Bisht, G.: Representing northern peatland microtopography and hydrology within the Community Land Model, *Biogeosciences*, 12, 6463–6477, <https://doi.org/10.5194/bg-12-6463-2015>, 2015.
- Spencer, R. G. M., Aiken, G. R., Wickland, K. P., Striegl, R. G., and Hernes, P. J.: Seasonal and spatial variability in dissolved organic matter quantity and composition from the Yukon River basin, Alaska, *Global Biogeochem. Cy.*, 22, GB4002, <https://doi.org/10.1029/2008GB003231>, 2008.
- Spencer, R. G. M., Mann, P. J., Dittmar, T., Eglinton, T. I., McIntyre, C., Holmes, R. M., Zimov, N., and Stubbins, A.: Detecting the signature of permafrost thaw in Arctic rivers, *Geophys. Res. Lett.*, 42, 2830–2835, <https://doi.org/10.1002/2015GL063498>, 2015.
- Striegl, R. G., Dornblaser, M. M., McDonald, C. P., Rover, J. A., and Stets, E. G.: Carbon dioxide and methane emissions from the Yukon River system, *Global Biogeochem. Cy.*, 26, 2012GB004306, <https://doi.org/10.1029/2012GB004306>, 2012.
- Taillardat, P., Bodmer, P., Deblois, C. P., Ponçot, A., Prijac, A., Ri-ahi, K., Gandois, L., del Giorgio, P. A., Bourgault, M. A., Tremblay, A., and Garneau, M.: Carbon Dioxide and Methane Dynamics in a Peatland Headwater Stream: Origins, Processes and Implications, *J. Geophys. Res. Biogeo.*, 127, e2022JG006855, <https://doi.org/10.1029/2022JG006855>, 2022.

- Tfaily, M. M., Hamdan, R., Corbett, J. E., Chanton, J. P., Glaser, P. H., and Cooper, W. T.: Investigating dissolved organic matter decomposition in northern peatlands using complimentary analytical techniques, *Geochim. Cosmochim. Acta*, 112, 116–129, <https://doi.org/10.1016/j.gca.2013.03.002>, 2013.
- Tfaily, M. M., Corbett, J. E., Wilson, R., Chanton, J. P., Glaser, P. H., Cawley, K. M., Jaffé, R., and Cooper, W. T.: Utilization of PARAFAC -Modeled Excitation-Emission Matrix (EEM) Fluorescence Spectroscopy to Identify Biogeochemical Processing of Dissolved Organic Matter in a Northern Peatland, *Photochem. Photobiol.*, 91, 684–695, <https://doi.org/10.1111/php.12448>, 2015.
- Tfaily, M. M., Wilson, R. M., Cooper, W. T., Kostka, J. E., Hanson, P., and Chanton, J. P.: Vertical Stratification of Peat Pore Water Dissolved Organic Matter Composition in a Peat Bog in Northern Minnesota: Pore Water DOM composition in a peat bog, *J. Geophys. Res. Biogeo.*, 123, 479–494, <https://doi.org/10.1002/2017JG004007>, 2018.
- Tipping, E., Billett, M. F., Bryant, C. L., Buckingham, S., and Thacker, S. A.: Sources and ages of dissolved organic matter in peatland streams: evidence from chemistry mixture modelling and radiocarbon data, *Biogeochemistry*, 100, 121–137, <https://doi.org/10.1007/s10533-010-9409-6>, 2010.
- Tiwari, T., Sponseller, R. A., and Laudon, H.: Extreme Climate Effects on Dissolved Organic Carbon Concentrations During Snowmelt, *J. Geophys. Res. Biogeo.*, 123, 1277–1288, <https://doi.org/10.1002/2017JG004272>, 2018.
- Tunaley, C., Tetzlaff, D., and Soulsby, C.: Scaling effects of riparian peatlands on stable isotopes in runoff and DOC mobilisation, *J. Hydrol.*, 549, 220–235, <https://doi.org/10.1016/j.jhydrol.2017.03.056>, 2017.
- Vonk, J. E., Tank, S. E., Mann, P. J., Spencer, R. G. M., Treat, C. C., Striegl, R. G., Abbott, B. W., and Wickland, K. P.: Biodegradability of dissolved organic carbon in permafrost soils and aquatic systems: a meta-analysis, *Biogeosciences*, 12, 6915–6930, <https://doi.org/10.5194/bg-12-6915-2015>, 2015.
- Ward, C. P. and Cory, R. M.: Complete and Partial Photo-oxidation of Dissolved Organic Matter Draining Permafrost Soils, *Environ. Sci. Technol.*, 50, 3545–3553, <https://doi.org/10.1021/acs.est.5b05354>, 2016.
- Weishaar, J. L., Aiken, G. R., Bergamaschi, B. A., Fram, M. S., Fujii, R., and Mopper, K.: Evaluation of Specific Ultraviolet Absorbance as an Indicator of the Chemical Composition and Reactivity of Dissolved Organic Carbon, *Environ. Sci. Technol.*, 37, 4702–4708, <https://doi.org/10.1021/es030360x>, 2003.
- White, M.: Modèle de développement des tourbières minérotrophes aqualysées du Haut-Boréal québécois, Université Laval, Québec, 78 pp., orpus ID: 135205929, 2011.
- Wickham, H.: ggplot2 Elegant Graphics for Data Analysis, Springer International Publishing, Cham, <https://doi.org/10.1007/978-3-319-24277-4>, 2016.
- Wilson, H. F. and Xenopoulos, M. A.: Effects of agricultural land use on the composition of fluvial dissolved organic matter, *Nat. Geosci.*, 2, 37–41, <https://doi.org/10.1038/ngeo391>, 2009.
- Worrall, F., Gibson, H. S., and Burt, T. P.: Production vs. solubility in controlling runoff of DOC from peat soils – The use of an event analysis, *J. Hydrol.*, 358, 84–95, <https://doi.org/10.1016/j.jhydrol.2008.05.037>, 2008.
- Worrall, F., Moody, C. S., Clay, G. D., Burt, T. P., and Rose, R.: The flux of organic matter through a peatland ecosystem: The role of cellulose, lignin, and their control of the ecosystem oxidation state: Flux of Organic Matter Through a Peat, *J. Geophys. Res. Biogeo.*, 122, 1655–1671, <https://doi.org/10.1002/2016JG003697>, 2017.
- Yu, Z. C.: Northern peatland carbon stocks and dynamics: a review, *Biogeosciences*, 9, 4071–4085, <https://doi.org/10.5194/bg-9-4071-2012>, 2012.